CHAPTER 2.1

Modeling the Brain

Michael A. Arbib
University of Southern California Brain Project and Computer Science Department, University of Southern California, Los Angeles, California

Abstract

Our work on developing Neuroinformatics tools and exemplary databases has been accompanied by a vigorous program of computational modeling of the brain. Amongst the foci for such work have been:

1. *Parietal-premotor interactions in the control of grasping:* We have worked with empirical data on the monkey from other laboratories and designed and analyzed PET experiments on the human to explore interactions between parietal cortex and premotor cortex in the control of reaching and grasping in the monkey, linking the analysis of the monkey visuomotor system to observations on human behavior.
2. *Basal ganglia:* We have examined the role of the basal ganglia in saccade control and arm control as well as sequential behavior and the effects of Parkinson's disease on these behaviors.
3. *Cerebellum:* We have modeled the role of cerebellum in both classical conditioning and the tuning and coordination of motor skills.
4. *Hippocampus:* Both neurochemical and neurophysiological investigations of long-term potentiation (LTP) have been related to fine-scale modeling of the synapse; we have also conducted systems-level modeling of the role of rat hippocampus in navigation, exploring its interaction with the parietal cortex. Our work on modeling mechanisms of navigation also includes a motivational component linking the role of hippocampus to a number of other brain regions.

This chapter provides a brief introduction to our systems-level modeling efforts. Chapter 2.2 presents the NSL Neural Simulation Language which has been the vehicle for much of our modeling at the level of systems neuroscience. Chapter 2.3 presents the EONS methodology for multi-level modeling, with particular attention to modeling synapses and the fine structures which constitute them, while Chapter 2.4 presents the Synthetic PET method which provides the bridge from neural modeling of large-scale neural systems to the data of brain imaging. Our Brain Models on the Web (BMW) model repository provides documentation (BMW is described in Chapter 6.2; the documentation of the models is on our Website), links to empirical data, and downloadable code for almost all the models described in this chapter.

2.1.1 Modeling Issues

Building on Arrays of Neurons

Brain Theory (Arbib, 1995) includes the use of computational techniques to model biological neural networks, but it also includes attempts to understand the brain and its function in terms of structural and functional" "networks" whose units are at scales both coarser and finer than that of the neuron. Modeling work for USCBP includes development of diverse models, many of which are incorporated in a database, Brain Models on the Web (BMW), which will advance Brain Theory.

While much work on artificial neural networks focuses on networks of simple discrete-time neurons whose connections obey various learning rules, most work in brain theory now uses continuous-time models that represent either the variation in average firing rate of each neuron or the time course of membrane potentials. The models also address detailed anatomy and physiology as well as behavioral data to feed back to biological

experiments. As we saw in the "Levels of Detail in Neural Modeling" section in Chapter 1.1, the study of a variety of connected "compartments" of membrane in dendrite, soma, and axon can help us understand the detailed properties of individual neurons, but much can still be learned about the large-scale properties of interconnected regions of the brain by modeling each region as a set of subpopulations ("arrays") using the *leaky integrator* model for each neuron. As shown before, in this case the internal state of the neuron is described by a single variable, the *membrane potential, m*(*t*), at the spike initiation zone. The time evolution of $m(t)$ is given by the differential equation:

$$\tau \frac{dm(t)}{dt} = -m(t) + \sum_i w_i X_i(t) + h$$

with resting level h; time constant τ, $X_i(t)$ the firing rate at the i^{th} input; and w_i the corresponding synaptic weight. This model does not compute spikes on an individual basis – firing when the membrane potential reaches threshold – but rather defines the *firing rate* as a continuously varying measure of the cell's activity, approximated by a simple, sigmoid function of the membrane potential, $M(t) = \sigma(m(t))$.

Connections between these two-dimensional arrays of neurons are defined in terms of interconnection masks which describe the synaptic weights. Consider the following equation where A, B, and C are arrays of neurons and W is a 3×3 connection mask (Fig. 1b). The equations:

$$\tau_A = 10\text{ms}$$
$$S_A = C + W^* B$$

state that the membrane time constant for A, τ_A, is 10 msec, and that for each cell i,j in array A, the cell's input, $S_A(i,j)$, is the sum of the output of the i,j^{th} cell in C plus the sum of the outputs of the 9 cells in B centered at i,j times their corresponding weights in W. That is,

$$sv_j = \sum_{k=-d}^{d} w_{jk}\ uf_{j+k}$$

Thus, the *operator in "W^*B" indicates that mask W is spatially convolved with B.

Chapter 1.1 provides references to a number of alternative strategies for modeling neurons, but this is the level for much of the modeling in the USC Brain Project. A notable exception is the detailed modeling of synapses and subsynaptic components using the EONS methodology of Chapter 2.3, but it is the" "system → regions → arrays of leaky integrator neurons" that has dominated our modeling and motivated the approach to modular, object-oriented neural systems embodied in our NSL Neural Simulation Language (Chapter 2.2).

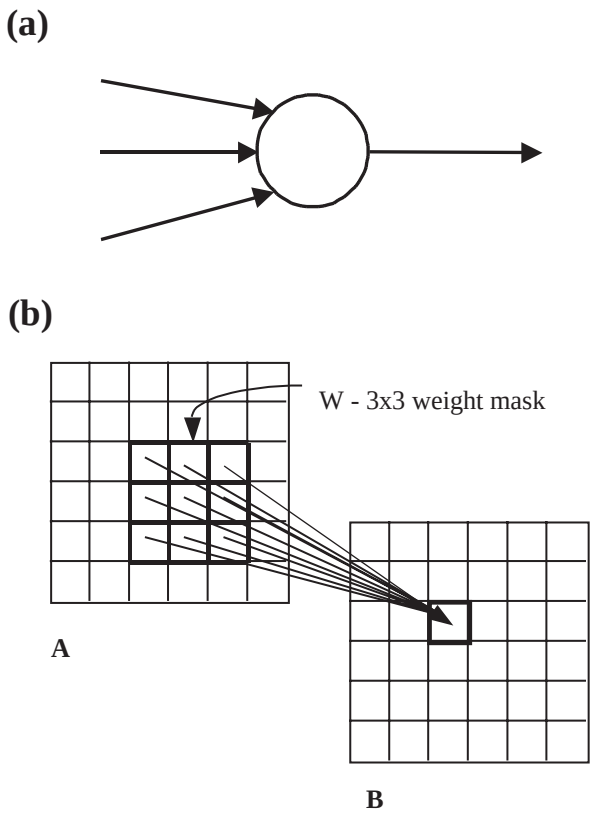

Figure 1 **(a)** An illustration of a basic neuron. A neuron receives input from many different neurons (*Sm*) which can affect the neuron's membrane potential (*m*), but it has only a single output (*M*), its firing rate. **(b)** Diagram showing the relationship between two arrays of neurons. In a uniformly connected network, each neuron in an array receives its inputs through the same synaptic weight mask. Here, the weight mask W applies a spatial convolution to input to B from a single array A, producing the result, $B = W^*A$. In general, the input to an array can come from many other arrays, each via its own mask.

Integration of Modeling and Experimentation

Analysis in neuroscience often goes to the extreme of focusing on one circuit or brain region and trumpeting it as "the" circuit implementing some specific function X, just as if we were to claim that Broca's area is "the" region for language. The other extreme is "holism," stressing that X may involve dynamic activity integrating all areas of the brain. Holism may be correct but seems to be useless as a guide to understanding. Our preferred approach is a compromise. We stress that any "schema" (see below) or function X involves the cooperative computation of many neural circuits (see Chapter 3 of Arbib *et al.*, 1998), but we then proceed by using a survey of the literature to single out a few regions for which good data are available correlating neural activity with the performance of function X. We then seek the best model available (from the literature, by research in our own group, or by a combination of both) which can yield a causally complete neural model that approximates both the patterns of behavior seen in animals performing X and the neural activity observed during these

performances. As time goes by, the model may yield more and more insight into the data on X (some of which may be new data whose collection was prompted by the modeling), whether by conducting new analyses of the model, increasing the granularity of description of certain brain regions, or extending the model to include representations of more brain regions. Other challenges come from integrating separate models developed to explain distinct functions X, Y, and Z to derive a single model of interacting brain regions able to serve all these functions. As we come to understand more fully the roles of particular brain regions in serving particular functions, we can then turn to more extensive models. However, I fear that if we try to model" "everything all at once" we will understand nothing, as the map would then be co-extensive with the whole territory (Borges, 1975).

In the "Hierarchies, Models, and Modules" section of Chapter 1.1, we presented the following methodology:

For each brain region, a survey of the . . . data calls attention to a few basic cell types. . . . The modeler . . . then creates one array of cells for each such cell type. The data tell the modeler what the activity of the cells should be in a variety of situations, but in many cases experimenters do not know in any quantitative detail the way in which the cell responds to its synaptic inputs, nor do they know the action of the synapses in great detail. In short, the available empirical data are not rich enough to get a model that would actually compute and so the modeler has to make a number of hypotheses about some of the unknown connections, weights, time constants, and so on to get the model to run. The modeler may even have to postulate cell types that experimenters have not yet looked for and show by computer simulation that the resulting network will indeed perform in the observed way when known experiments are simulated, in which case (1) it must match the external behavior; and (2) internally, for those populations that were based on cell populations with measured physiological responses, it must match those responses at some level of detail. What raises the ante is that (1) the modeler's hypotheses suggest new experiments on neural dynamics and connectivity, and (2) the model can be used to simulate experiments that have never been conducted with real nervous systems.

These ideas have motivated the efforts on Model Repositories and Summary Databases described in Part 6 of this volume, where we describe work to date on developing an environment that supports the linkage of data and models in the development, testing, and versioning of models. However, to date the development of models and the new modeling environment have proceeded in parallel. The result is that the models described below were developed "by hand" and then inserted into BMW. In the future, models will more and more be developed using the tools and environments of the NeuroInformatics Workbench to support the increased integration of modeling and experimentation.

Models, Modules, Schemas, and Interfaces

In general, we view a model as comprising a single "top-level module" composed of a number of different modules, which themselves may or may not be further decomposable. If a module is decomposable, we say this "parent module" is decomposed into submodules known as its "child modules;" otherwise, the module is a "leaf module."

Modules as Brain Structures

Fig. 1 of Chapter 1.1 (reproduced as Fig. 7 below) illustrated the modular design of a model by showing in (a) a basic model of reflex control of saccades involving two main modules, each of which is decomposed into submodules, with each submodule defining an array of physiologically defined neurons; (b) embedded this basic model into a far larger model which embraces various regions of cerebral cortex, thalamus, and basal ganglia. While the model may indeed be analyzed at this top level of modular decomposition, (c) showed how to further decompose basal ganglia to tease apart the role of dopamine in differentially modulating the direct and indirect pathways. This example introduces the case where the modules correspond to some physical structure of the brain – whether a brain region, an array of neurons, a neuron, or some subcellular structure. Here I want to emphasize two other kinds of module.

Modules as Schemas

In modeling some complex aspect of the brain, we may want to use a detailed structural description for some parts of the model and functional descriptions for others. For example, in modeling the role of a parietal area in visually directed grasping, we may choose not to burden our model with a detailed representation of the actual brain regions (retina, thalamus, visual cortex, etc.) that process the visual input it receives but instead combine their functionality in a single abstract *schema*. In other cases, we may decompose a schema into finer schemas and simulate their interaction; some but not all of these subschemas will be mapped onto detailed neural structures. The starting point for schema theory as used here (Arbib, 1981) was to describe perceptual structures and distributed motor control in terms of coordinated control programs linking simpler perceptual and motor schemas, but these schemas provide the basis for more abstract schemas which underlie action, perception, thought, and language more generally.

In summary (see Arbib *et al.*, 1998, chap. 3), the functions of perceptual-motor behavior and intelligent action of animals situated in the world can be expressed as a network of interacting schemas. Each schema itself involves the integrated activity of multiple brain regions. A multiplicity of different representations – whether they be partial representations on a retinotopic basis, abstract representations of knowledge about types of

object in the world, or more abstract "planning spaces" – must be linked into an integrated whole. Such linkage, however, may be mediated by distributed processes of "cooperative computation" (competition and cooperation). There is no one place in the brain where an integrated representation of space plays the sole executive role in linking perception of the current environment to action. We thus see that the modules that constitute any one of our models of (some aspect of) the brain may be designed to represent an actual structure of the brain, or a schema which captures a function which may possibly require interaction of multiple brain structures for its realization.

Modules as Interfaces

The above types of modules represent the component structures and/or functions to be included in a model of some aspect of the brain. Other modules are designed to help the user interact with the model. For example, in the "Schematic Capture" section of Chapter 1.1, we related the key notion of an *experimental protocol* – which defines a class of experiments by specifying a set of experimental manipulations and observations – to the use of a *simulation interface* which represents an experimental protocol in a very accessible way, thus making it easy for the non-modeler to carry out experiments on a given model. Fig. 2 of Chapter 1.1 illustrated a particular user interface comprising two modules: One allows the user to set conditions for a particular simulation run of the model and to control the execution of that run; the other is a display module, showing the results of the simulation. The simulation interface allows one to explore hypotheses as to how specific cells work together to produce overall behavior and may also be understood as samplings of the interaction of multiple neural arrays, thus deepening our understanding of cellular activity from the systems point of view.

2.1.2 Parietal-Premotor Interactions in the Control of Grasping

This section presents the FARS (Fagg-Arbib-Rizzolatti-Sakata) model for grasping. It is named for the modelers Andy Fagg and myself and for the experimentalists Giacomo Rizzolatti and Hideo Sakata, whose work anchors the model. The model shows show how a view of an object may be processed to yield an appropriate action for grasping it and explains the shifting patterns of neural activity in a variety of brain regions involved in this visuomotor transformation.

The neurophysiological findings of the Sakata group on parietal cortex (Taira *et al.*, 1990) and the Rizzolatti group on premotor cortex (Rizzolatti *et al.*, 1988) indicate that parietal area AIP (the anterior intra-parietal sulcus) and ventral premotor area F5 in monkey (Fig. 2) form key elements in a cortical circuit which transforms visual information on intrinsic properties of objects into hand movements that allow the animal to grasp the objects appropriately (see Jeannerod *et al.*, 1995, for a review). Motor information is transferred from F5 to the primary motor cortex (denoted F1 or M1), to which F5 is directly connected, as well as to various subcortical centers for movement execution. Discharge in most F5 neurons correlates with an action; the most common are grasping with the hand, grasping with the hand and the mouth, holding, manipulating, and tearing. Rizzolatti *et al.* (1988) thus argued that F5 contains a "vocabulary" of motor schemas (Arbib, 1981). The situation is in fact more complex, and" "grasp execution" involves a variety of loops and a variety of other brain regions in addition to AIP and F5.

Affordances (Gibson, 1979) are features of an object or environment relevant to actionvisual processing may exploit them to extract cues on how to interact with an object or move in the environment, complementing processes for categorizing objects or determining their identity. The FARS model (Fagg and Arbib, 1998) provides a computational account of what we call the *canonical system*, centered on the AIP $\rightarrow$ F5 pathway, showing how it can account for basic phenomena of grasping. The highlights of the model are shown in Figs. 3 and 4. Our basic view is that AIP cells encode *affordances for grasping* from the visual stream and send their neural codes on to area F5. As Fig. 3 shows, some cells in AIP are driven by feedback from F5 rather than by visual inputs so that AIP can monitor ongoing activity as well as visual affordances. Here we indicate the case in which the visual input has activated an affordance for a precision pinch, with AIP activity driving an F5 cell pool that controls the execution of a precision pinch.

What we show, however, is complicated by the fact that the circuitry is not for a single action, but for a behavior designed by Sakata to probe the time dependence of activity in the monkey brain. In the Sakata paradigm, the monkey is trained to watch a manipulandum until a go signal instructs it to reach out and grasp the object. It must then hold the object until another signal instructs it to release the object. In Fig. 3, cells in AIP instruct the set cells in F5 to prepare for execution of the Sakata protocol using a precision pinch. Activation of each pool of F5 cells not only instructs the motor apparatus to carry out the appropriate activity (these connections are not shown here), but also primes the next pool of F5 neurons (i.e., brings the neurons to just below threshold so they may respond quickly when they receive their own go signal) as well as inhibiting the F5 neurons for the previous stage of activity. Thus, the neurons that control the extension phase of the hand shaping to grasp the object are primed by the set neurons, and they reach threshold when they receive the first go signal, at which time they inhibit the set neurons and prime the flexion neurons. These pass threshold when receiving a signal that the hand has reached its maximum

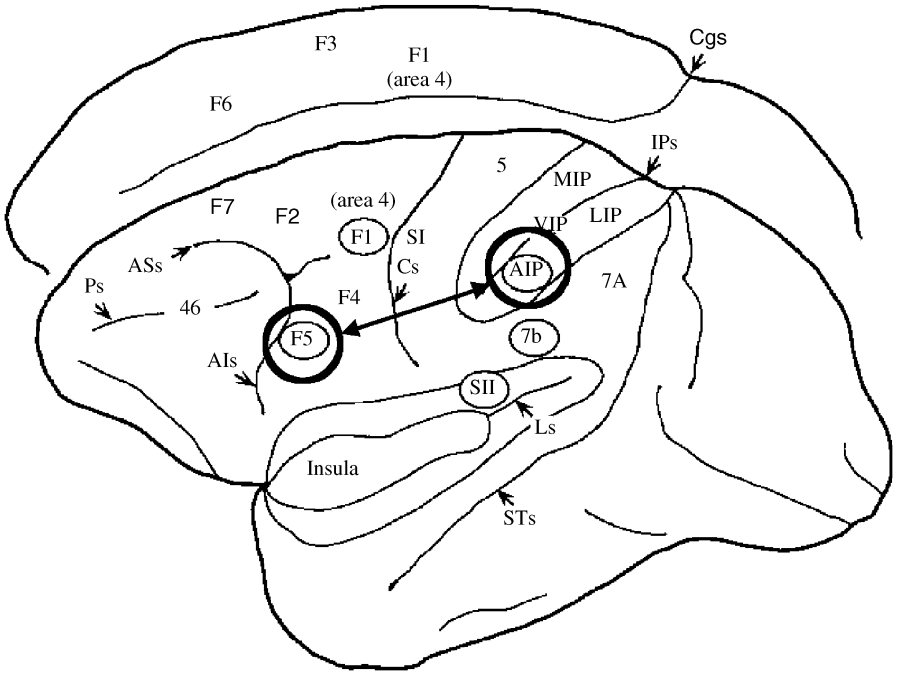

Figure 2 A side view of the left hemisphere of the Macaque monkey brain dominates the figure, with a glimpse of the medial view of the right hemisphere above it to show certain regions that lie on the inner surface of the hemisphere. The central fissure is the groove separating area SI (primary somatosensory cortex) from F1 (primary motor cortex, more commonly called MI). Frontal cortex is the region in front of (in the figure, to the left of) the central sulcus. Area F5 of premotor cortex (i.e., the area of frontal cortex just in front of primary motor cortex) is implicated in the elaboration of "abstract motor commands" for grasping movements. Parietal cortex is the region behind (in the figure, to the right of) the central sulcus. The groove in the middle of the parietal cortex, the intra-parietal sulcus, is shown opened here to reveal various areas. AIP (the anterior region of the intra-parietal sulcus) processes visual information relevant to the control of hand movements and is reciprocally connected with F5.

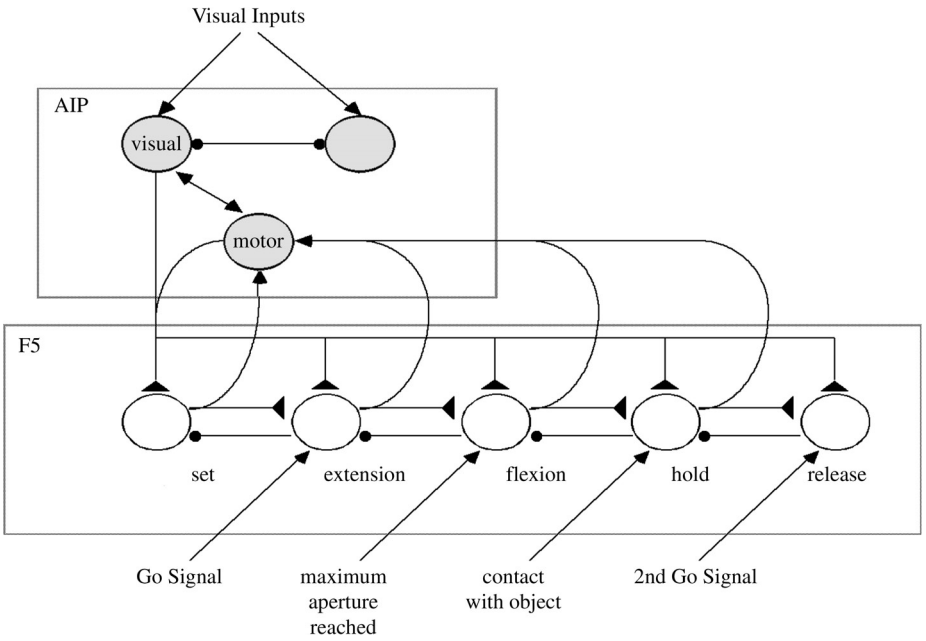

Figure 3 Hypothesized information flow in AIP and F5 in the FARS model during execution of the Sakata paradigm. This neural circuit appears as a rather rigid structure; however, we do not hypothesize that connections implementing the phasic behavior are hardwired in F5. Instead, we posit that sequences are stored in pre-SMA (a part of the supplementary motor area) and administered by the basal ganglia.

aperture. The hold neurons, once primed, will become active when receiving a signal that contact has been made with the object, and the primed release neurons will command the hand to let go of the object once they receive the code for the second go signal.

Karl Lashley (1951) wrote of "The Problem of Serial Order in Behavior," a critique of stimulus-response approaches to psychology. He noted that it would be impossible to learn a sequence such as A, B, A, C as a stimulus-response chain because the association "completing A triggers B" would then be interfered with by the association "completing A triggers C" or would dominate it to yield an infinite repetition of the sequence A, B, A, B, ... The generally adopted solution is to segregate the learning of a sequence from the circuitry that encodes the unit actions, the latter being F5 in the current study. Instead, another area has neurons whose connections encode an "abstract sequence" Q1, Q2, Q3, Q4, with sequence learning then involving learning that activation of Q1 triggers the F5 neurons for A, Q2 triggers B, Q3 triggers A again, and Q4 triggers C. In this way, Lashley's problem is solved. Other studies lead us to postulate that the storage of the sequence may be in the part of the supplementary motor area called pre-SMA (Luppino *et al*., 1993) with administration of the sequence (inhibiting extraneous actions while priming imminent actions) carried out by the basal ganglia (Bischoff, 1998; Bischoff-Grethe and Arbib, 2000).

We now turn to the crucial role of the inferotemporal cortex (IT) and prefrontal cortex (PFC) in modulating F5's selection of an affordance (Fig. 4). Here, the dorsal stream (from primary visual cortex to parietal cortex) carries, among other things, the information needed for AIP to recognize that different parts of the object can be grasped in different ways, thus extracting affordances for the grasp system which (according to the FARS model) are then passed on to F5, where a selection must be made for the actual grasp. However, the dorsal stream does not know "what" the object is; it can only see the object as a set of possible affordances. The ventral stream (from primary visual cortex to inferotemporal cortex), by contrast, is able to recognize what the object is. This information is passed to the prefrontal cortex, which can then, on the basis of the current goals of the organism and recognition of the nature of the object, bias F5 to choose the affordance appropriate to the task at hand. In particular, the FARS model represents the way in which F5 may accept signals from areas F6 (pre-SMA), 46 (dorsolateral prefrontal cortex), and F2 (dorsal premotor cortex) to respond to task constraints, working memory, and instruction stimuli, respectively (see Fagg and Arbib, 1988, for more details).

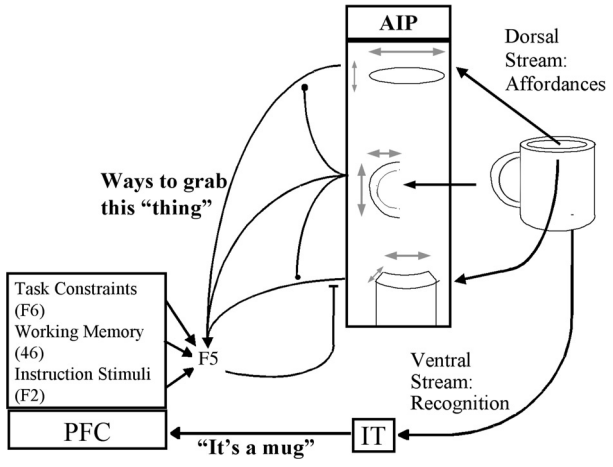

Figure 4 The role of inferotemporal cortex (IT) and prefrontal cortex (PFC) in modulating the F5′ selection of an affordance.

Synthetic PET

In Chapter 2.4, we will introduce the Synthetic PET method for analyzing simulation results obtained with a large-scale neural network model to predict the results of human brain-imaging experiments. In particular, we will describe Synthetic PET predictions based on the FARS model, their testing by studies using positron emission tomography (PET) imaging of human subjects, and the new insights that can be gained when modeling can use Synthetic PET to integrate findings from neurophysiology and neuroanatomy of monkey with brain imaging of human. Such studies both build on and contribute to our understanding of the homologies between brain regions of different species (Chapter 6.4).

2.1.3 Basal Ganglia

Control of Saccades

An early success in neural modeling came with the work of David Robinson and others who explained how the brain stem could serve as a saccade burst generator, acting as a control system to convert the current "error" in gaze (the angle between the direction of gaze and the position of a visual target) into, first, the motor neuron firing required for the burst of muscle activity that would turn the eye to the desired position and, second, the tonic activity to hold the eye in that position (see Robinson, 1981, for a review). The resultant control model was significant in that many of the variables could be related to the firing of specific classes of neurons in the brainstem; however, the early models were defective in that the position of the target was represented by a single error variable, rather than by the position of the target as imaged onto the retina. Thus, later models (e.g., Scudder, 1988) interposed a model of the superior colliculus as the device which could serve as the" "retinotopic mapper" converting position on the retina (retinotopy) into the sort of signal that could be used by the brainstem saccade burst generator.

Further studies had to address new data which showed an essential role for cerebral cortex in a variety of more complex behaviors. For example, a monkey can be trained not to respond to a target while a fixation light is on but then to saccade to the position of the target at the end of the fixation even if the target is no longer visible. This requires an additional" "schema" for target memory. Other data showed that if the animal is exposed to two targets of during the fixation period, then at the offset of the fixation he will saccade to the two targets in turn. Moreover, the neural representation of the second target after the first saccade is completed corresponds to the retinotopic coding that the second target would have had after the first saccade (but did not have, because it was no longer visible after that saccade had occurred). This requires yet another schema, this one for "remapping." The extension of the basic model thus required is shown in Fig. 5.

Dominey and Arbib (1992) used an extensive analysis of the literature to replace the schema model of Fig. 4 by the NSL model outlined in Fig. 6. Heavy outlines separate modules representing different brain regions, and each brain region is divided into arrays motivated by physiological data. For example, there are cells in different regions whose activity is best correlated with the onset of a saccade; other cells have activity best correlated with maintained activity or working memory between the presentation of a stimulus at the beginning of a delay period until the actual response. However, as noted earlier when discussing our general methodology, while a great deal of knowledge of the available data went into the construction of the model, the data are not rich enough to get a model that would actually compute so we, as modelers, had to make a number of hypotheses about missing connections, weights, and time constants to get the model to run. The model was then tuned so that the passage from the presentation of visual input to generation of eye movement matches the external behavior, and internally (for those populations that were based on cell populations with measured physiological responses), we match, at some level of detail, those responses. In particular, the model detailed how thalamocortical loops could implement target memory (which is thus a schema whose implementation is distributed across interacting brain regions), while remapping was conducted by circuitry intrinsic to the region LIP of posterior parietal cortex (shown as PP in Fig. 6), whose projections then accounted for related activity patterns in other brain regions. In particular, the model then showed how, when a new target representation was created by remapping, the result would replace the old representation in target memory.

A new model for the role of the basal ganglia (BG) in the control of saccades (Crowley, 1997) is shown in Fig. 7 (already shown as Fig. 1 of Chapter 1.1). The new model was motivated by two different issues, and our response to each issue illustrates the modular methodology of our approach to large-scale neural modeling. One was that new data about many different parts of the brain had been found during the early 1990s and we wanted to reflect those data in the model. There were certain hypotheses we made that proved to be robust, while there are others that are no longer consistent with the available data. For example, new data on superior

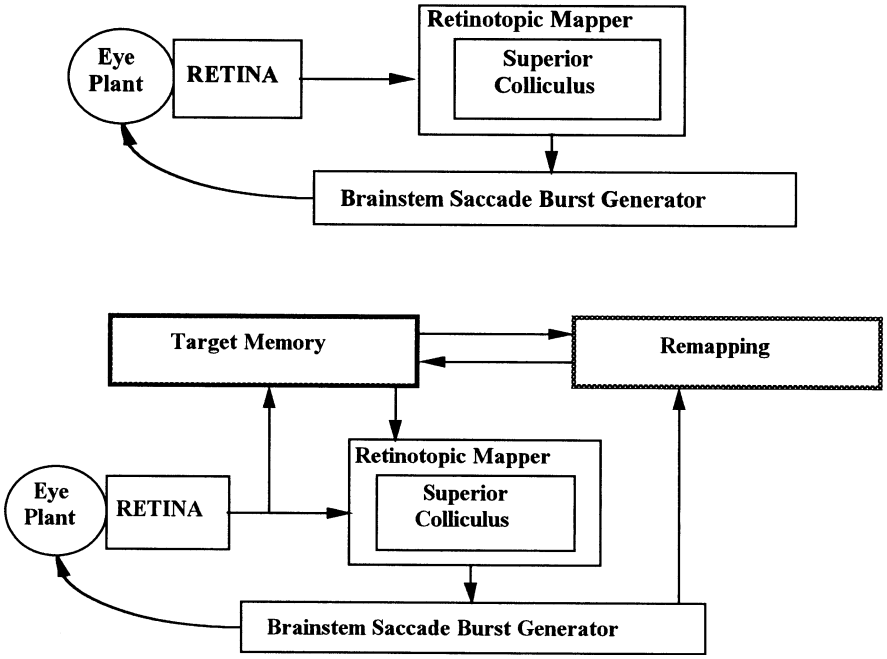

Figure 5 **(Top)** A modular description of *structures* involved in the reflex control of saccades. **(Bottom)** Extending the modular description which adds *schemas* for *Target Memory* and *Remapping* necessary to account for a variety of studies of saccades in monkeys.

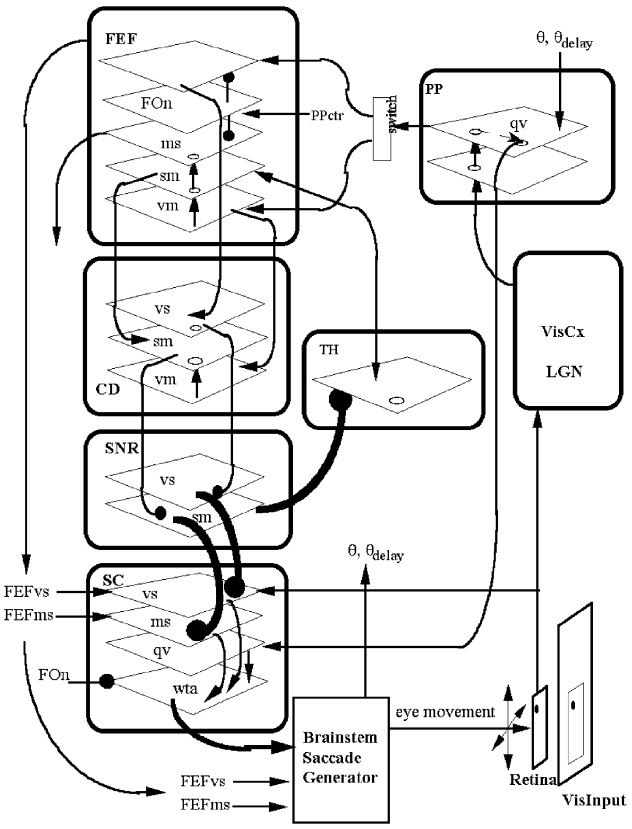

Figure 6 The modular design of the NSL model developed by Dominey and Arbib (1992) to explain the neural mechanisms for memory saccades and double saccades. The model includes the superior colliculus and brainstem, as well as cortical regions, thalamus, and basal ganglia. It represents each brain region by one or more layers of physiologically identified cell types. vs. = visual pre-saccade, ms = memory pre-saccade, sm = sustained memory, vm = visual response to memory target, qv = quasi-visual, wta = winner take all, PPctr = central element of PPqv, FEF = frontal eye fields, PP = posterior parietal cortex, CD = caudate nucleus, SNR = substantia nigra pars reticulata, SC = super colliculus, TH = thalamus (mediodorsal), Fon = fovea on (foveation).

colliculus led us to replace the superior colliculus of the Dominey-Arbib model by the one shown in Fig. 7a. The other was that we had earlier focused on data on normal function, but now we wanted to look at dysfunction. In particular, we wished to understand how dopamine depletion in the basal ganglia leads to the symptoms of Parkinson's disease. To this end, we extended the model of the direct pathway through the basal ganglia of the Dominey-Arbib model to include the indirect pathway and to model the differential effects of dopamine, providing a detailed representation of circuitry for all the regions shown in Fig. 7c. Fig. 8 shows one result obtained with this model. The graphical output shows saccade velocity in the double saccade task. The normal behavior of the model is on the left; on the right, we see the effect of cutting the dopamine in half in the model. By modeling the differential effect of the direct and indirect pathways within the basal ganglia, we find that with reduced dopamine there is only one saccade. This begins to give us some insight into the bradykinesia and akinesia that are seen in Parkinson patients, as well as tying in with some of the available monkey data.

This work not only extended our analysis of a variety of brain regions, it also led (in USCBP work that used the Crowley model as a testbed for work on both NSL and BMW) to an important example of using the explicit description of an experimental protocol to design a simulation interface which allows non-expert users to easily conduct related simulation experiments. Fig. 2 of Chapter 1.1 shows the simulation interface for the double saccade protocol in which a monkey fixates a fixation point, during which time two brief targets are briefly flashed. After the fixation point is removed, the monkey saccades to the remembered position of the two targets in turn. The simulation interface contains two panels: one to set up and run the experiment, the other to observe a variety of displays of neural activity.

Control of Sequential Arm Movements

The modeling result of Fig. 8 is consistent with the finding that patients with diseases of the BG, particularly Huntington's disease and Parkinson's disease, do not have significant motor control difficulties when visual input is available (Bronstein and Kennard, 1985) but do have problems with specific forms of internally driven *sequences* of movements (Curra *et al.*, 1997). This implies that the basal ganglia may be involved in assisting cortical planning centers in some fashion as well as providing sequencing information for cross-modal movements (e.g., simultaneous arm reach, hand grasp, head movement, and eye movement). We have thus extended the model of Fig. 7b to include the control of arm movements as well as saccades (Fig. 9). In each case, the *direct path*, involving projections directly from the striatum onto the BG output nuclei, is primarily responsible for providing an estimate of the next sensory state, based upon the current sensory state and the planned motor command, to cortical planning centers. The primary role of the *indirect path*, where the striatum projects onto the external globus pallidus (GPe), in turn projecting to the subthalamic nucleus (STN) and finally to the BG output structures, is to inhibit motor activity while cortical systems are either determining which motor command to execute or are waiting for a signal indicating the end of a delay period.

Because microstimulation of thalamic pallidal receiving areas tends not to elicit arm movement (Buford *et al.*, 1996), the basal ganglia may not so much control the precise dynamics of movement as permit a movement to be made. That is, the disinhibition of the thalamus may increase the thalamic firing rate which in turn may provide the cortical regions enough input to reach threshold and fire. Without this disinhibition, which appears to be lacking in Parkinson's disease, cortical cells have a more

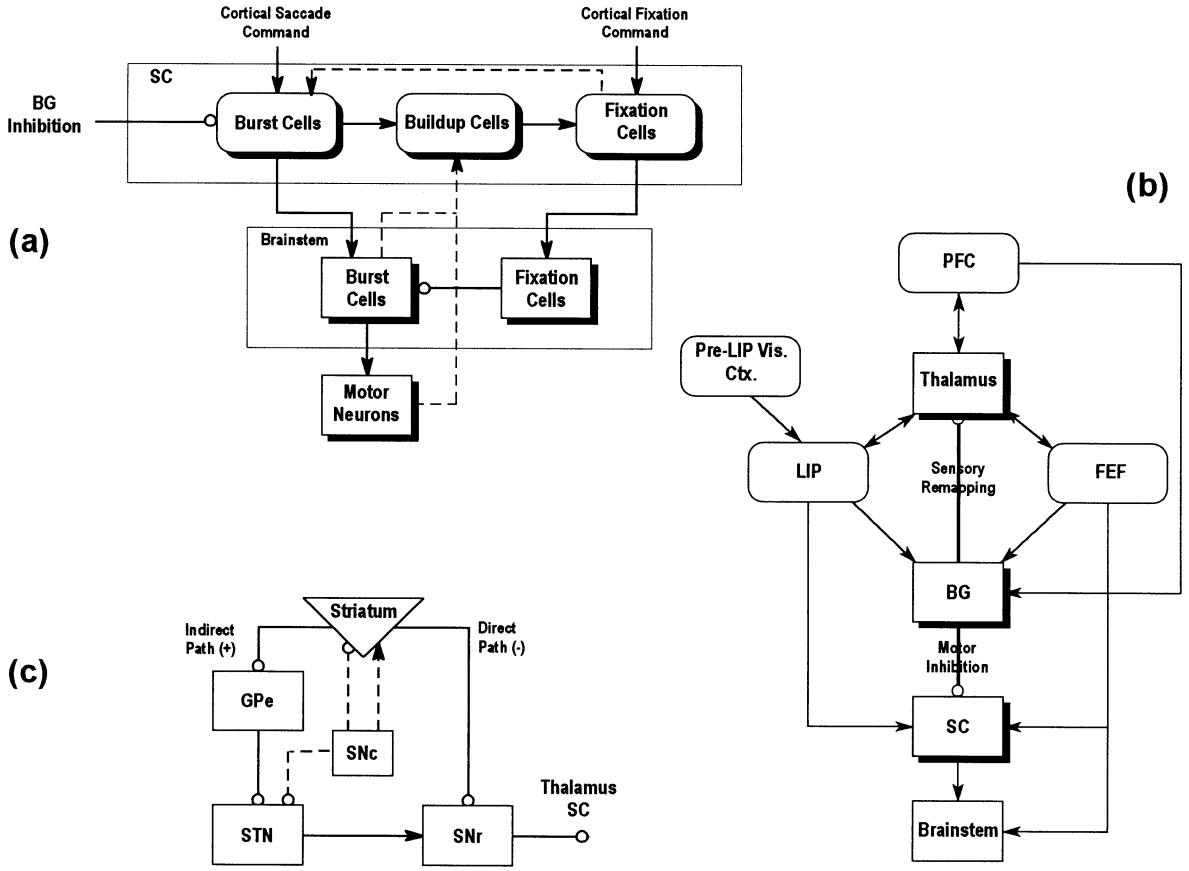

Figure 7 **(a)** A basic model of reflex control of saccades involves two main modules, one for superior colliculus (SC) and one for brainstem. Each of these is decomposed into submodules, with each submodule defining an array of physiologically defined neurons. **(b)** The model of (a) is embedded into a far larger model which embraces various regions of cerebral cortex (represented by the modules Pre-LIP Vis. Ctx., LIP, PFC, and FEF), thalamus, and basal ganglia. While the model may indeed be analyzed at this top level of modular decomposition, we need to further decompose BG, as shown in **(c)** if we are to tease apart the role of dopamine in differentially modulating (the two arrows shown arising from SNc) the direct and indirect pathways within the basal ganglia (Crowley, 1997).

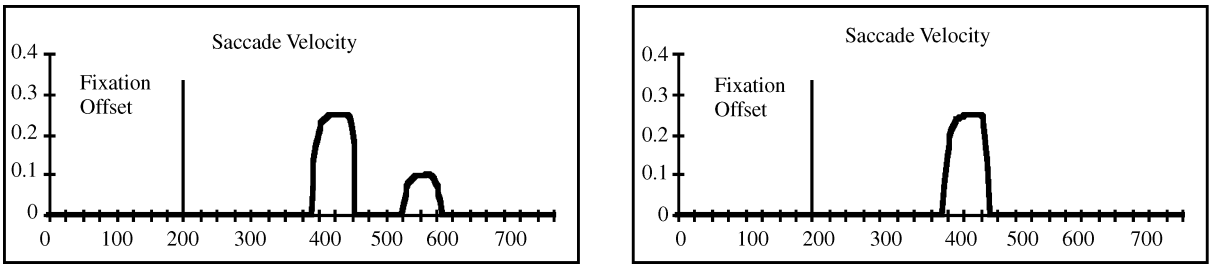

Figure 8 Double saccades with dopamine manipulation. Cutting dopamine in half caused a second saccade not to be generated due to increased inhibition in the SNr (substantia nigra pars reticulata) medial circuit of the model.

difficult time achieving threshold, leading to difficulties in movement performance. In Huntington's disease, therefore, one might suggest that too much thalamic disinhibition allows for indiscriminate motor activity, as cortical cells more easily reach threshold.

Although Fig. 9 shows a generic cortical projection to basal ganglia, this projection is composed of different areas of cortex. The simple box marked "Cortex" becomes a complex structure in our actual computer modeling, combining models of the prefrontal cortex (PFC), frontal eye fields (FEF), and the lateral intraparietal cortex (LIP) in our saccade model and two subregions of the supplementary motor area (SMA)pre-SMA and SMA-proper in our model of limb movements. Because we have already discussed the oculomotor system in some detail, we now focus on control of sequences of skeletomotor actions (Bischoff, 1998; Bischoff-Grethe and Arbib, 2000). Within the skeletomotor pathway, PFC is responsible for working memory and for sequence learning (Barone and Joseph, 1989; Jenkins

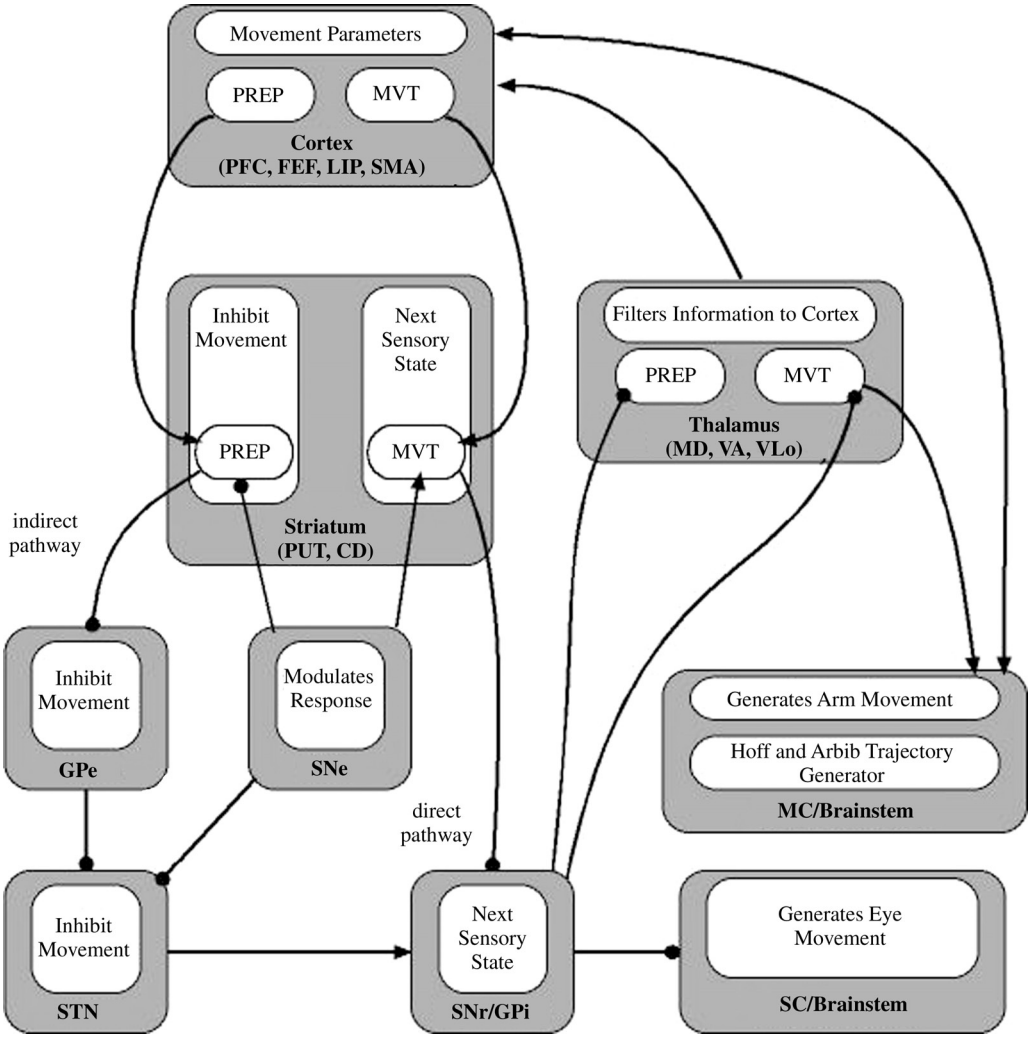

Figure 9 Model showing proposed functions for each component of the oculomotor and skeletomotor circuit. Although we have only shown the brain stem as divided into the movement-specific regions, we also follow the "loop hypothesis" that all other regions are subdivided into relatively distinct regions forming the separate oculomotor and skeletomotor circuits. Our key hypothesis is the shared functionality of the corresponding regions in the two circuits. GPe = external globus pallidus; Gpi = internal globus pallidus; MC = motor cortex; MVT = movement neurons; PREP = premovement neurons; SC = superior colliculus; SNc = substantia nigra pars compacta; SNr = substantia nigra pars reticulata; STN = subthalamic nucleus.

et al., 1994). PFC projects to the pre-supplementary motor area (pre-SMA). Because pre-SMA is responsible for preparing a movement sequence, particularly if visually guided, PFC may be a source for the sequences that pre-SMA "knows." Pre-SMA projects sequential information to both SMA-proper and to the basal ganglia's indirect pathway. SMA-proper is involved in the internal generation of sequences and repetitive movements.

SMA-proper neurons contain information on the overall sequence to be performed, keep track of which movement is next and which movement is currently being performed, project the current movement to be performed to MC and to the direct pathway of the basal ganglia, and project the preparations of the next movement of the sequence to another population of premovement neurons within MC and to the indirect (inhibitory) pathway of basal ganglia. The motor cortex, then, carries out the motor command and handles the fine tuning of the movement (e.g., target position, amplitude, force) partly based upon information provided by the basal ganglia. The motor cortex projects the motor parameters to both the brain stem and the basal ganglia's direct pathway. We postulate that the basal ganglia's two pathways perform two different roles: the indirect pathway inhibits upcoming motor commands from being performed while the current movement is in progress, while the direct pathway projects the next sensory state back to cortex. This informs SMA-proper and MC of the expected next state and allows these regions to switch to the next movement of the sequence.

In using this model to perform sequential movements (Bischoff, 1998; Bischoff-Grethe and Arbib, 2000), we provided the model with the location of three targets

and the order in which contact should be made. SMA-proper contained neurons similar to those seen by Tanji and Shima (1994) representing an overall task sequence and the subsequences within the task. A trajectory generator (Hoff and Arbib, 1992) performed the movements as dictated by MC. Under normal conditions, the model successfully moved from target to target and exhibited a velocity similar to normal subjects. When we depleted dopamine, we encountered several behavioral results. As SNc reduced its ability to affect the direct and indirect pathways, there was an increase in the firing rates of STN and both sections of globus pallidus. The increase in inhibitory output led to a decrease in the MC firing rate, as MC was unable to completely overcome GPi's inhibition via ventrolateral pars oralis thalamus (VLo) projections. This reduced firing rate translated to a slower movement time. Thus, the natural balance between the two pathways is disturbed when dopamine is lost. In Parkinson's disease, this leads to an increase in activation of the indirect pathway (movement inhibition) and a decrease in effectiveness of the direct pathway (next sensory state). We also saw a slowdown in overall neural activity the basal ganglia and the motor cortex took longer to reach peak firing rates. The slowdown in neural activity, coupled with the increased inhibition of movement, was responsible for pauses between movements within the sequence. We therefore began to see pauses between movements from one target to the next; however, we also found that for each subsequent movement, the velocity was less. This is similar to the bradykinesia seen in Parkinson's disease patients when asked to trace the edges of a polygon (Agostino *et al*., 1992). The model also exhibited a reduction in cortical firing rates. When dopamine was further depleted, the model was capable of performing only the movement towards the first target, reminiscent of the situation shown in Fig. 8. This model has also been used to reproduce results seen in normal and Parkinson's disease subjects in a reciprocal aiming task and normal behavior during conditional elbow movements (Bischoff, 1998).

2.1.4 Cerebellum

The architecture of the cerebellar circuitry is by and large well understood, as are the relationships between the cerebellum and other brain structures. The functions of the cerebellum include the learning of fine control of motor coordination and classical conditioning of motor responses, and it is widely believed that the same type of synaptic plasticity (i.e., a long-term depression, LTD, of synaptic transmission between the parallel fibers and the Purkinje cells in cerebellar cortex) is involved in both adaptation of skeletomotor and oculomotor skills and in learning of classically conditioned motor responses. The hypothesis postulates that repeated pairing of appropriate stimulus patterns reaching Purkinje neurons through the mossy fiber/parallel fiber pathways, with activation of the single climbing fiber which activates the Purkinje cell, results in LTD of the parallel fiber to Purkinje neurons synapses. However, the relative contribution of the cerebellar cortex and the deep cerebellar nuclei to the learning of skill and classical conditioning tasks has not been clearly understood. In particular, it has been proposed that a long-term potentiation (LTP) of synaptic transmission between the mossy fibers and the neurons of the deep cerebellar nuclei also contributes to such learning. In the models reported here, however, we concentrate on the parallel fiber to Purkinje neurons synapses as the loci of synaptic change.

Cerebellar Models of Motor Control and Coordination

Our models of cerebellar involvement in motor control hypothesize that the cerebellum does not act directly on the muscles but rather acts through motor pattern generators (MPGs) – circuits which combine, for example, trajectory or rhythmic control with local feedback circuitry. We view the cerebellum (combining cerebellar cortex and cerebellar nuclei) as being divided into *microcomplexes*. Each microcomplex is a general, modular computational module comprising a patch of cerebellar cortex and nuclear cells whose basic form is shown in Fig. 9. We do *not* hypothesize that the cerebellar microcomplex learns to *replace* the MPG but rather that the complex learns how to adjust its output to appropriately tune and augment the output of the MPG to which it belongs. Each microcomplex combines a patch of cerebellar cortex (Purkinje cells and Golgi cell) with the underlying set of cells in the cerebellar nucleus to which the Purkinje cells project and the inferior olive cells, which provide the climbing fibers that control learning by providing error signals in our models of motor learning and the CS (conditioned stimulus) in our models of classical conditioning Fig. 10. The "contextual input" is provided by the parallel fibers (each of which crosses a number of microcomplexes), the granule cell axons which provide a nonlinear combination of mossy fiber inputs. The job of the Purkinje cells is to learn to pair the parallel fiber output with a pattern of inhibition of the nuclear cells so as to ensure that these cells better tune the MPGs.

As Fig. 11 shows, the parallel fibers are long enough that their shared "contextual input" Purkinje cells may learn not only to tune individual MPGs to changing circumstances but also to coordinate multiple MPGs (such as those for reaching and grasping) so that a complex movement may be achieved in a smooth and integrated way. In short, we view the cerebellum as applying its compensations by modulating MPGs, whether cortical or subcortical, and this compensation occurs on multiple time scales. Further, the compensation patterns can

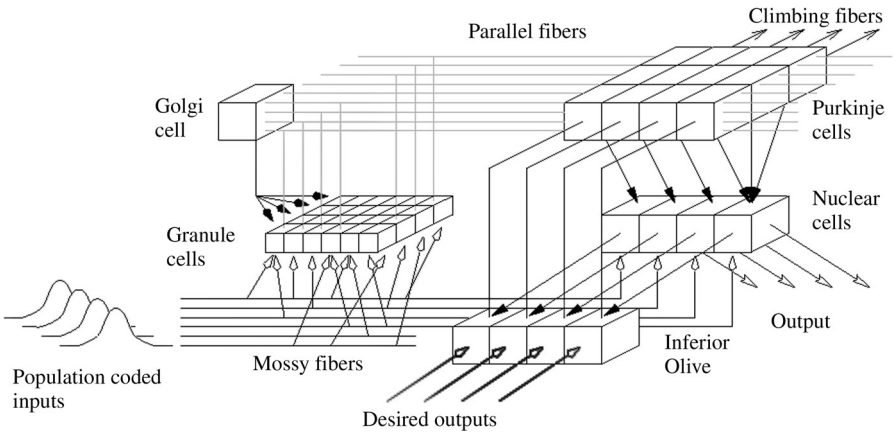

Figure 10 The microcomplex combines a patch of cerebellar cortex (Purkinje cells and Golgi cell) with the underlying set of cells in the cerebellar nucleus, to which the Purkinje cells project, and the inferior olive cells, which provide the climbing fibers which control learning. The parallel fibers (each of which crosses a number of microcomplexes) are the granule cell axons that provide a nonlinear combination of mossy fiber inputs. The job of the Purkinje cells is to learn to pair the parallel fiber output with a pattern of inhibition of the nuclear cells so as to ensure that these cells better tune the MPGs.

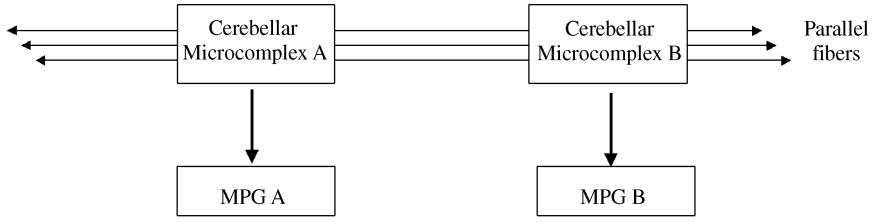

Figure 11 Hypothesis: The cerebellum adjusts the parameters of MPGs both to tune individual MPGs and to coordinate related MPGs.

be stored and recalled based on higher level task information. The critical test of the cerebellum is its ability to effectively compensate for complex nonlinear dynamics and to adapt that compensation as the dynamics change. Thus, a cerebellar model must be tested and developed in conjunction not only with an MPG model but also with a "plant model" which contains sufficient complexity to "challenge" the cerebellum model. However, we shall not get into the biomechanics in this chapter.

Our model posits a structure in which a microcomplex of cerebellar cortex and underlying cells forms the key module, but in this case we build a model system that integrates sensory-motor information for intersegmental coordination and nonlinear dynamic compensation. These microcomplexes in turn drive, tune, and coordinate motor pattern generators to create descending signals that impinge on motor neurons.

Schweighofer *et al.* (1996a,b), in modeling the role of cerebellum in prism adaptation and compensating for dysmetria in saccades, developed a computational model of the" "microcomplex" and showed how the microzone could act by adjusting the parameters of a motor pattern generator outside the cerebellum (in this case, in the brain stem). Schweighofer *et al.* (1998a) and Schweighofer *et al.* (1998b) showed how the cerebellum may compensate for Coriolis forces and other joint interactions in allowing coordinated control of multiple joints in reaching. Our saccade and throw models included no inhibitory interneurons in cerebellar cortex, but our reach model has brought in Golgi cells, basket cells, and stellate cells with realistic firing rates and interconnections. In this study, the model of the Purkinje cells has gone beyond the relatively simple leaky integrator neuron to include a set of spiking dendrites, so we are well on the way to combining a systems level view of cerebellar function with detailed cellular analysis (Fig. 12).

Arbib *et al.* (1994, 1995) were inspired by discussion of the data that have now been written up by Martin *et al.* (1996). This experimental work showed that prism adaptation for throwing a ball or dart involves (1) the cerebellum, and (2) (and this is the exciting part) task-specific sensorimotor transformations rather than a global adaptation of the visual field. Our work explained how this could take place, using the microcomplex developed in the saccade studies but now modulating a motor controller in premotor cortex. To ground our discussion of the role of cerebellum in motor control, we will devote the next section to an outline of the follow-up modeling conducted by Spoelstra and Arbib (1997). We then turn to a brief discussion of classical conditioning, but first we

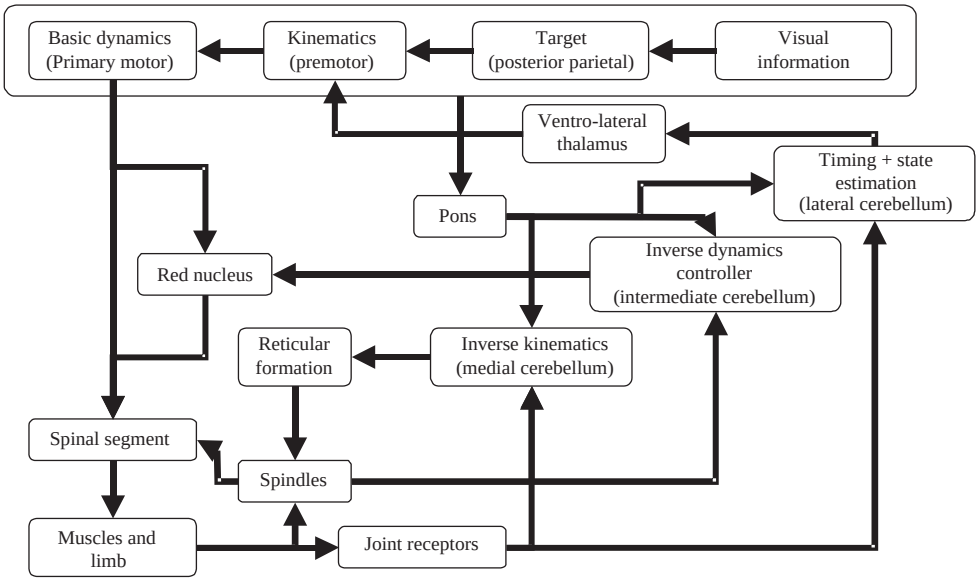

Figure 12 Diagram indicating the many components necessary to understand the interaction of cerebellum (with different parts involved in postural control and dynamic compensation), cerebral cortex, subcortical regions, spinal reflex circuitry, and the biomechanics of muscles and limb in the adaptive control of limb movements. (See Spoelstra *et al.*, 2000, for details.)

need to discuss the synaptic plasticity rule used in the models.

What is distinctive about the Purkinje cell is its two principal kinds of input. There are on the order of a hundred thousand parallel fibers, each making a single synapse with the Purkinje cell, and a single climbing fiber, which makes so many synapses with the Purkinje cell that a single spike arriving on a climbing fiber will cause the Purkinje cell to fire several times. Both Marr (1969) and Albus (1971) suggested that the climbing fiber provides the error signal for training the synapses from parallel fibers to Purkinje cells, so the Purkinje cell could learn to classify patterns of parallel fiber firing and thus of the states that these firings encoded. Where Marr suggested that the coincidence of parallel fiber and climbing fiber activity would yield an increase in the synaptic weight, Albus postulated that there would be a decrease. These conjectures inspired a great deal of work, first neurophysiological then neurochemical, by Masao Ito and his colleagues (see Ito, 1984, for a review) which finally established that the Albus hypothesis was correct: Active climbing fiber input to a Purkinje cell signals that any active parallel fiber synapse on that Purkinje cell should be weakened. What Ito and others in fact established was a phenomenon of long-term depression (LTD), a lowering of synaptic strength lasting several hours. In fact, modeling considerations have shown that this must be balanced by some form of long-term potentiation (LTP) to stop all synaptic strengths from drifting down towards 0 over time.

We later refined the Marr-Albus-Ito perspective not only by introducing equations that balance LTP and LTD, but also by attending to the fact that the delay between motion generation and error detection implies the need for a *short-term memory local to each synapse* to retain the locus of cerebellar activity involved in the movement. We posited that parallel fiber activity provides a synapse with a "window of eligibility" for modification of all synaptic strength on receipt of a climbing fiber input which peaks at about 200 msec, corresponding to the typical delay between the time the firing of a Purkinje cell modulates the generation of a movement and the time that the climbing fiber reports back to the cell on the visually sensed error in the movement. More detailed modeling shows that this eligibility can be represented by the concentration of a molecular species called a *second messenger* within the given synapse – with the concentration of the messenger largest for synapses involved in the movement related to the current climbing fiber "error signal."

What is of particular interest from a modeling perspective about this model is that a purely system-level model – linking overall human behavior to arrays of relatively simple neurons – led us to consider timing issues which then required us to modify our learning rules. This modification of the synapse adjustment rule then led us to consider new ideas about the possible neurochemistry of synaptic plasticity in the cerebellum. The model shows how work at one level of a hierarchy of levels for competition neuroscience can either depend on or will be stimulated by work at another. We thus see the linkage of data and modeling from the systems level to the neurochemical level, a key feature of the USC Brain Project. Moreover, because an IO cell typically spikes from only 2 to 6 times a second, it is inappropriate

to represent its behavior by an average firing rate, so we instead use an integrate-and-fire model which explicitly generates spikes to be used in the synaptic learning rule.

Prism Adaptation for Throwing

A basic component of adaptive behavior is the adaptation of sensori-motor transformations. Prism adaptation is a paradigm for such adaptation, and the cerebellum is required for this. BMW includes a biologically based neural net model of this role of cerebellum (Spoelstra and Arbib, 1997), which builds on our earlier work (Arbib *et al*., 1994). The database for this modeling includes much data on the anatomy and physiology of cerebellum and other regions involved in motor control, as well as a body of behavioral data. The work of Martin *et al*. (1995, 1996) on prism adaptation of human eye-hand coordination in a number of throwing tasks shows the task specificity of the adaptation, as well as its dependence on the cerebellum. The behavior of interest here is the perturbation that we see in throwing a ball or dart at the target when a person puts on a pair of prism glasses (Fig. 13a). Most people are able to adjust over a number of trials, but this adaptation seems to be missing in people with certain types of cerebellar damage. A subject throws at a target, then dons 30° wedge prism glasses, causing him to throw 30° off target. With repeated throws, the subject improves until he once again throws on target. When the prisms are removed, the subject misses by almost 30° on the opposite side and has to readjust his aim. Fig. 13b shows that the model is able to reproduce this behavior. The systems-level circuit of the model is shown in Fig. 14.

It is beyond the scope of this overview to elaborate upon the details of the model, save to note that the cerebral cortex provides information about both where the arm is to be aimed during the throw and whether or not the subject is wearing prisms and uses this information to control throwing. The cerebellum samples the same information to provide an adaptive side loop that can modify this cortical control. As in other NSL models, brain regions are represented as two-dimensional arrays of neurons, and neurons (other than the inferior olive neurons) are modeled as leaky integrators with a positive real-valued output representing the instantaneous firing rate of the neuron.

What goes on in prism adaptation? One hypothesis is that it provides a global visual transformation, compensating for the global shift of the visual input provided by the prism; however, the data of Martin *et al*. suggest a set of "private" visuomotor transformations. Prism adaptation for throwing with the left hand does not transfer to throwing with the right hand. Even for throwing with the right hand, adaptation to prism throwing for throwing overarm will not transfer at all to underarm throwing in some subjects, will transfer slightly in others, and will transfer almost completely in others. The model of Spoelstra and Arbib reproduces this by varying the degree of overlap between the microcomplexes involved in overarm and underarm throwing, thus giving us new insight into the relation between sensory processing and motor control.

Classical Conditioning

The Thompson Laboratory at USC focuses on basic associative learning and memory using classical (Pavlovian) conditioning of discrete behavioral responses (e.g.,

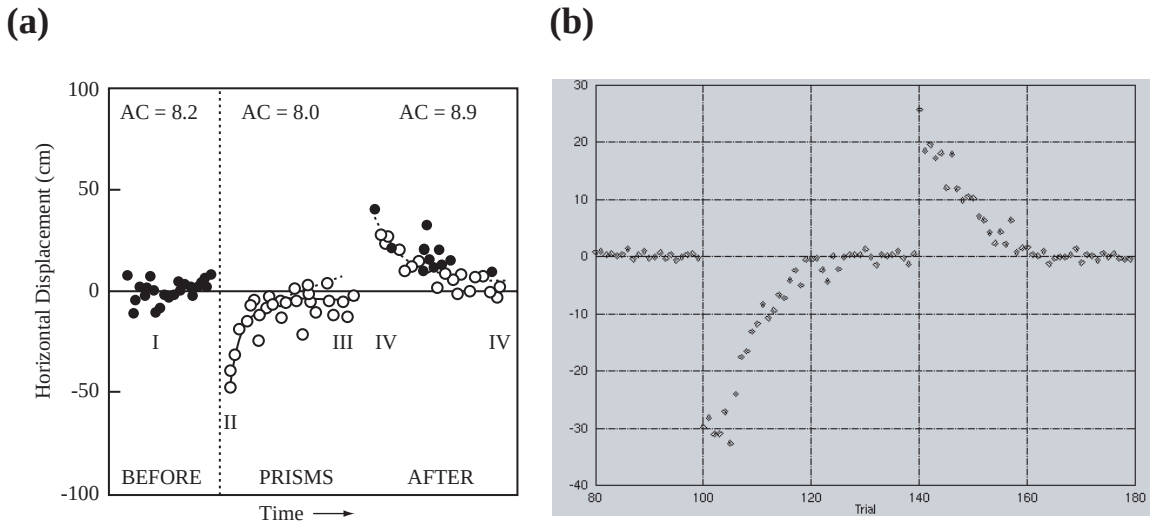

Figure 13 **(a)** Empirical data showing the accuracy of throwing in successive trials before donning prisms, then while wearing the prisms, and finally after doffing the prisms. Note the process of re-learning after removal of the prisms. **(b)** Reproduction of this behavior by the model in which adaptation is mediated by the cerebellum.

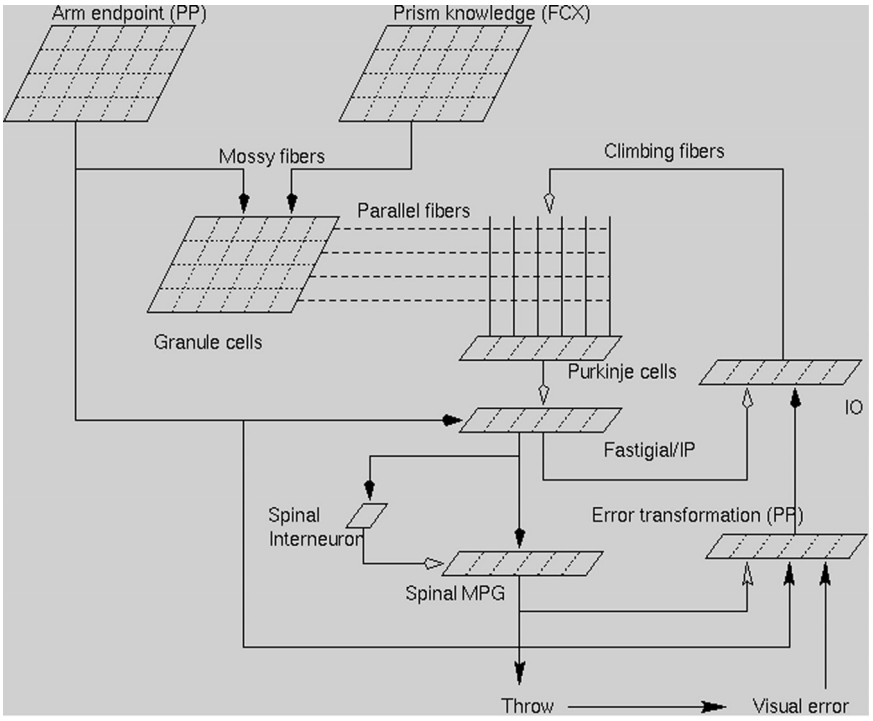

Figure 14 The structure of the prism adaptation model, based on the microcomplex of Fig. 10.

eyeblink) as a model system. They find that the cerebellum is essential for this form of learning and memory under all conditions. The hippocampus is not necessary for basic conditioning, but it is essential for *trace conditioning*, where the conditioned stimulus (CS) – in Thompson's study, a tone – ends before the unconditioned stimulus US – in Thompson's study, an airpuff to the rabbit eyeball – begins. If the unconditioned or training stimulus is sufficiently aversive, learned fear will develop associated with the CS and involving the amygdalar and hippocampal systems. The modeling of the eyeblink system described here focuses on how the cerebellar system learns to make specific behavioral responses that are most adaptive in dealing with the aversive event. In comparing our models of motor control to those for classical conditioning, we still view the cerebellar microcomplex as the building block for our modeling but now view the climbing fiber signal as the unconditioned stimulus (US) rather than the error signal. In a way, of course, an aversive US *is* an error signal—it is a mistake not to blink before the airpuff hits the eyeball.

This observation highlights the crucial role of *timing* in motor control, even when the controlled system is as apparently simple as an eyeblink. In his USCBP Ph.D. thesis, Jeffrey Grethe (1999) addressed the data in the NeuroCore database on classical conditioning by modeling the cerebellar microcomplex as a Hebbian cell assembly and studying its role in the production of the well-timed conditioned response (CR). We close our discussion of cerebellum with a review of this work and related models and data.

In Grethe's model (Fig. 15), the cerebellar cortex receives mossy fiber input from both pontine nuclei and recurrent projections from the interpositus nucleus, with the recurrent projection much smaller than the pontine sensory projection. The cerebellar cortex in the microcomplex, therefore, consists of two distinct populations of granule cells: those influenced by the recurrent mossy fiber connections from the deep nuclei and those that are not. Golgi cells in the cerebellar cortex inhibit granule cells surrounding that Golgi cell (Ito, 1984). In the microcomplex, both of the granule cell populations are inhibited by a Golgi cell that receives its input from the mossy fibers as well as the parallel fibers from the granule cells themselves. The Purkinje cells in the basic unit of the microcomplex receive input from both granule cell populations.

The interpositus consists of two cell populations: excitatory and inhibitory cells. Both the excitatory and inhibitory interpositus neurons generate recurrent collaterals within the nucleus; however, the excitatory cells generate the recurrent collateral projection to the cortex. In the microcomplex, the excitatory cells receive mossy fiber input and recurrent excitatory input as well as an inhibitory input from the Purkinje cell and the inhibitory interpositus neurons. The inhibitory interpositus cells of the microcomplex receive input from the excitatory cells and in turn inhibit these excitatory cells. This basic architecture allows the recurrent excitation in the excitatory interpositus cell to be modulated by the Purkinje cell in the cerebellar cortex. Each group of cells modeled in the cerebellar microcomplex is a "lumped" collection of

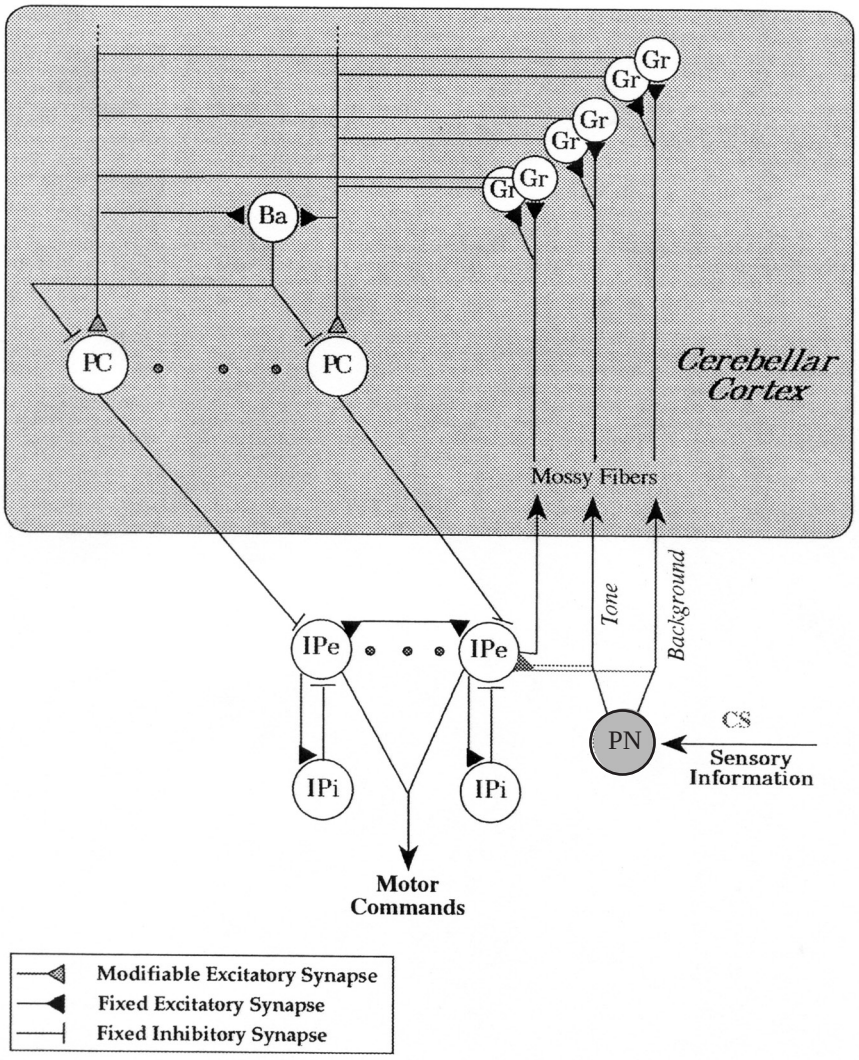

Figure 15 Cerebellar cell assembly. Recurrent activity in the cerebellum, between the cerebellar cortex and interpositus nucleus, is initiated and controlled by the cerebellar cortex. Sensory information is relayed to the cerebellar cortex and the interpositus nucleus through the pontine nuclei.

neurons of that type. For example, a modeled recurrent granule cell neuron is actually a representation of a pool of those neurons. The architecture of the model tries to preserve the topographic projections between the cerebellar cortex and the deep nuclei as well as the beam-like organization of Purkinje cells receiving input from the parallel fibers. Each Purkinje cell population modeled represents such a collection of Purkinje cells located on a common beam of parallel fibers. This allows the cerebellar microcomplex to be broken down into columns of topographically organized cells.

In the model of the microcomplex, the mossy fiber input consists of both sensory information from the pontine nucleus and a recurrent projection from the interpositus nucleus. The sensory information from the pontine nucleus is separated into two projections, a tone-responsive mossy fiber projection and a tone-unresponsive mossy fiber projection. The response of the tone-responsive mossy fibers was modeled after the activity of neurons in the pontine nuclei elicited by acoustic stimuli (Aitkin and Boyd, 1978). The majority of the units responded only at the onset of the tone stimulus and responded with a high-frequency burst of activation. An increase in the firing rate is applied 10 msec after the onset of the tone stimulus, which is consistent with onset latencies reported by Steinmetz (1990). The mossy fiber inputs to the model are the only elements whose firing rate are predetermined. All other elements in the model are determined by their inputs and neuron properties. In the model, only the first column of cells in the microcomplex receives the tone stimulus.

Purkinje cells tend to have high tonic firing rates (Eccles *et al.*, 1967, 1971). Berthier and Moore (1986) found that in the awake rabbit the range of Purkinje cell

(a)

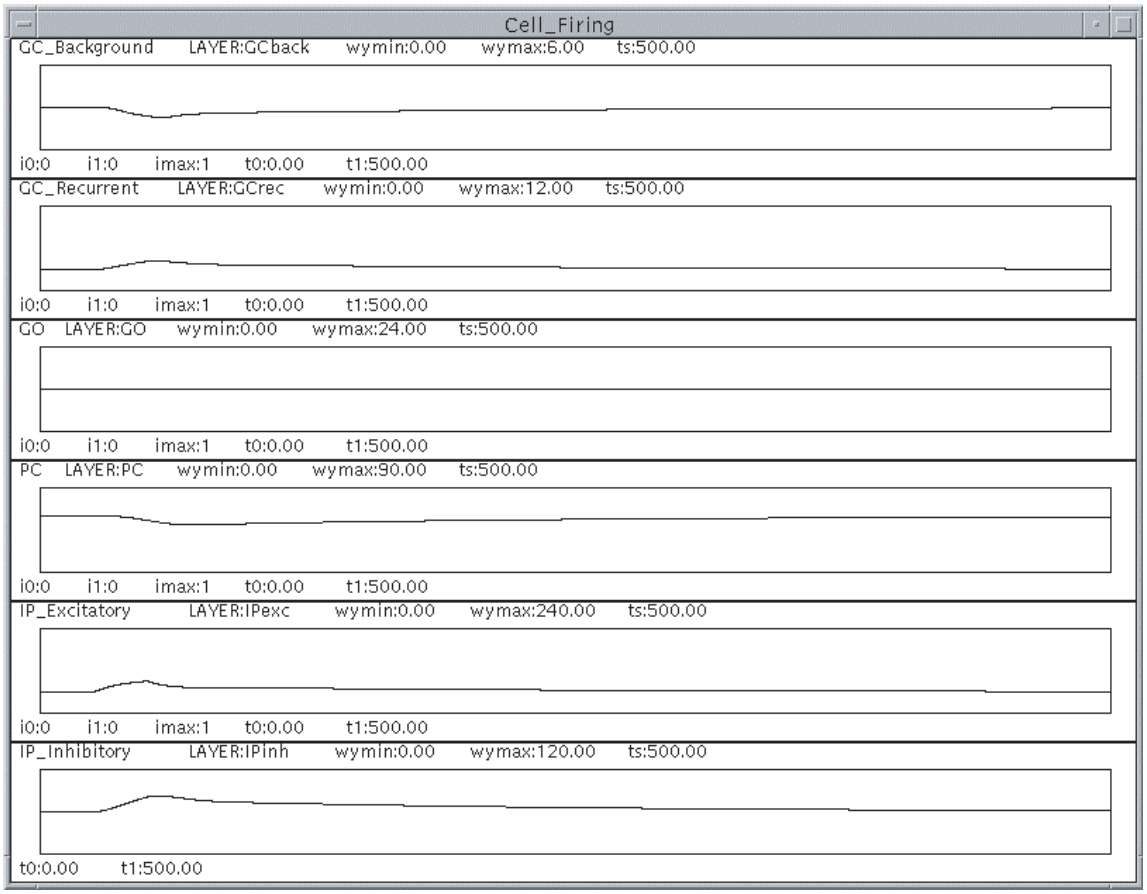

Figure 16 Model output of tone-responsive column. **(a)** Stability of cell assembly. A small stimulus was given that results in an initial activation of the cell assembly (as represented by the activity in the excitatory IP cell) that subsequently decays to background levels. **(b)** Bi-stability of cell assembly. In this example, a small stimulus was given that activates the cell assembly. After the stimulus onset, the activation of the recurrent feedback to the cerebellar cortex forces the Golgi cell to inhibit the granule cells and select the more active recurrent pathway. This example shows how the process of synaptic fatigue allows recovery from the activated state.

activity falls in the range of 40 to 100 Hz. In the model, the simulated Purkinje cell rate of 60 Hz falls well within this range. The high tonic activity of Purkinje cells is the result of integrating the low-frequency inputs from the granule cells. The tonic firing rate of neurons in the interpositus was 60 Hz, which corresponds to the mean rate of 60 Hz observed in awake rabbits.

Grethe did not study the actual learning process but sought to study what state of the microcomplex would support an appropriately timed conditioned response. The synaptic weights from the recurrent granule cell population to the Purkinje cell are assumed to have undergone LTD, whereas the synapses from the non-recurrent granule cell population are slightly potentiated. This normalization of the weights is necessary to keep the Purkinje cell firing normally during baseline activity. This synaptic normalization has been used in our other models of the cerebellum. The synaptic weights from the tone-responsive mossy fiber to tone-responsive interpositus cell has undergone LTP.

A microcomplex must be stable despite the inherent noisiness of the input as well as able to initiate itself given a salient enough input. To examine the issue of stability, a tone-responsive cerebellar microcomplex will be considered (i.e., the first column of cells in the microcomplex is tone responsive, all other columns are not). Given a weak input at 10 msec into the trial, the trained microcomplex shows no prolonged response (Fig. 16a). Once the stimulus terminates, the activity in the microcomplex (represented by the collective activation of the excitatory interpositus cells) returns to its baseline level; however, we need to be able to activate this microcomplex. In order to accomplish this, a nonlinear threshold must be present that allows the activity of the microcomplex to grow after this threshold has been reached. A candidate nonlinear characteristic was found in the Purkinje cell by Llinás and Mühltethaler (1988). If the input to the Purkinje cell drops below a certain level, the Purkinje cell ceases to fire. This nonlinearity is modeled in the cerebellar microcomplex by defining the proper squashing

(b)

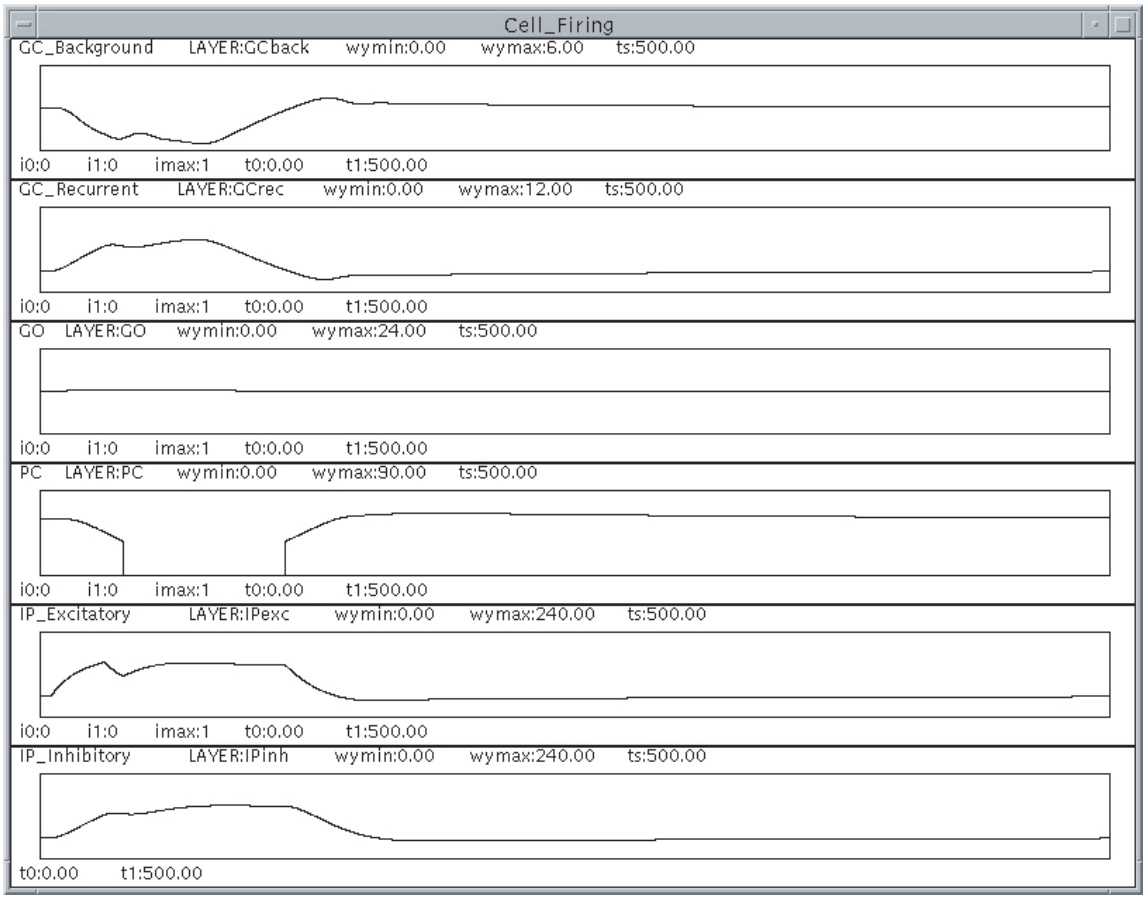

Figure 16 (*Continued*)

function for the Purkinje cell activity so that when the activity of the Purkinje cell falls below a certain threshold it ceases to fire.

Now, if a salient enough stimulus is given to the microcomplex, the microcomplex activates (Fig. 16b). This activation is controlled by the granule cell-Golgi cell network. Given a stimulus the excitatory interpositus cells activate the recurrent connection to the cerebellar cortex. If this activation is strong enough, the recurrent mossy fiber input to the recurrent granule cell population causes these granule cells to activate. This mossy fiber input and subsequent granule cell activation begins to activate the Golgi cell. It is important to note, however, that the Golgi cell activity varies only slightly from its baseline firing rate. This is due to the feedforward and feedback nature of its influence on the granule cells. The small tone-responsive input to the Golgi cell through the mossy fibers will only slightly activate the Golgi cell; however, this slight activation will already cause the Golgi cell to begin inhibiting the granule cell populations. The Golgi cell then, through its continued inhibitory influence on the granule cells, selects for the most active granule cell subpopulation the recurrent granule cell population. Because the parallel fiber synapses from the recurrent granule cell population to the Purkinje cell have been depressed relative to the synapses from the background granule cell population, the Purkinje cell begins to slow its firing rate. If this process is able to cause the Purkinje cell to reach the threshold where the neuron ceases firing, the microcomplex has then reached an activated state, which will allow the activity in the microcomplex to reverberate.

Once the microcomplex has been activated, however, a process must exist that is responsible for deactivating the microcomplex. Various mechanisms have been proposed to stop regenerative activity in the nervous system. Synchronized thalamocortical oscillations spontaneously appear and disappear. The appearance of these oscillations results from the activation of a small number of cells that in turn recruit a progressively larger number of neighboring neurons. These synchronized oscillations then cease spontaneously. This cessation of activity is partially due to a persistent activation of a hyperpolarization-activated cation conductance (Bal and McCormick, 1996); however, a more widely accepted phenomenon that could be responsible for the deactivation of a microcomplex is synaptic fatigue. Kaplan *et al.*

(1991) extended the notion of the microcomplex by including use-dependent synaptic fatigue. Experimental evidence exists that suggests that many synapses exhibit decreased efficacy with repeated use. The synaptic fatigue in the model is due to an activity-dependent depletion of synaptic resources in the excitatory interpositus neuron synapses. Once an excitatory interpositus cell has crossed a firing threshold where the resources for synaptic transmission can no longer be replenished, the synaptic efficacy of the synapses begins to decrease. The synaptic resources are then replenished once the neurons activity falls below a certain level and the resources are able to be replenished.

The microcomplex itself is stable in that it is able to return to its baseline firing characteristics after activation; however, in order to test the overall stability and robustness of the system, one has to look further. In order to evaluate the model, noise was injected at the level of the inputs to the model (i.e., because all activation in the model is derived from the inputs, noise added at this stage will affect all levels of processing). The model is actually very robust when noise is added to the system.

The microcomplex is now able to produce an activation in response to mossy fiber input, but how is the timing of this response controlled? Once the microcomplex has been initiated, the rest of the cells in the microcomplex must also activate to produce the response. Once a tone-responsive interpositus cell (in the first column) forces the first Purkinje cell to cease firing, the microcomplex is given the necessary recurrent excitatory drive to begin influencing other Purkinje cells in the microcomplex. This causes a cascade of Purkinje cells that cease to fire over a period of time. Each time a Purkinje cell shuts off, it endows the microcomplex with more excitatory drive that in turn causes more Purkinje cells to cease firing. This cascade in turn determines the timing and topography of the response of the interpositus neurons; therefore, the overall timing of the response is dependent upon the onset time of the Purkinje cell bi-stability. This bi-stability is controlled by the synaptic strength between the recurrent granule cell population and the Purkinje cell. When a column in the microcomplex activates, activation in the granule cell population shifts from a balanced state (all populations firing at their baseline levels) to one in which the recurrent granule cell population is firing at a higher rate, whereas the background granule cell population is firing at a lower rate. This allows the recurrent population to have a greater influence on the Purkinje cell. If the synapses in the projection are depressed (through a process such as LTD), then the Purkinje cell will not receive as much input and will begin to slow its firing rate. If this shift of balance continues long enough until the Purkinje cell reaches the bi-stability threshold, then that Purkinje cell will cease firing and release the system further to allow other Purkinje cells to follow. The overall timing of the response is, therefore, dependent on how quickly the Purkinje cells in the microcomplex reach this bi-stability threshold, which is dependent upon the synaptic strength (i.e., the level of synaptic depression at the recurrent granule cell to Purkinje cell synapse). The latencies are completely controlled by the level of depression in the recurrent granule cell to Purkinje cell projection (with more depression at 225 msec than at 400 msec). It is interesting to note that this implies that with learning (LTD) the microcomplex will produce activations at earlier and earlier latencies – the response will continue to move forward in time. This is what is actually observed in a typical classical conditioning experiment.

2.1.5 Hippocampus, Parietal Cortex, and Navigation

Our models of the roles of parietal cortex in saccades and grasping are firmly grounded in data from *monkey* neurophysiology and comprise networks of biologically plausible neurons implemented on computers, yielding many simulation results. By contrast, our models of the role of *rat* parietal cortex and hippocampus in navigation address data from rat neurophysiology but are strongly motivated by data from primate neurophysiology whose implications for analogous properties of the rat brain have yet to be tested.

Cognitive Maps and the Hippocampus

To use a road map, we must locate (the representations of) where we are and where we want to go, and then find a path that we can use as we navigate towards our goal. We use the term *cognitive map* for a mental map together with these processes for using it. Thus, the "place cells" found in rat hippocampal CA3 and CA1 (O'Keefe & and Dostrovsky, 1971) provide only a "you are here" signal, not a full cognitive map. Moreover, a given place cell will have a "place field" in a highly familiar environment, with up to 70% probability. This suggests that the hippocampus is dynamically tuned to a" "chart" of the current locale, rather than providing a complete "atlas" with a different place cell for every place in the rat's "entire world." This suggest two alternatives (at least):

1. The different "charts" are stored elsewhere and must be "reinstalled" in hippocampus as dictated by the current task and environment.
2. The cells of hippocampus receive inputs encoding task and environment which determine how sensory cues are used to activate a neural representation of the animal's locale.

In either case, we see that these "charts" are highly labile. Noting the importance of parietal systems in representing the personal space of humans, we seek to understand cognitive maps in a framework that embraces parietal cortex as well as hippocampus.

Although some hippocampal cells fire when rats drink water or approach water sources (Ranck, 1973), O'Keefe & and Conway (1978) did not find the role of food or water to be markedly different from other cues that identify the location of a place field. Eichenbaum *et al.* (1987) recorded from rats repetitively performing a sequence of behaviors in a single odor-discrimination paradigm and found *goal-approach cells* which fired selectively during specific movements, such as approach to the odor port or to the reward cup. Despite these and related findings, there is still no evidence that hippocampus proper can simultaneously encode the rat's current location and the goal of current navigation.

Taxon and Locale Systems: An Affordance Is Not a Map

O'Keefe & and Nadel (1978) distinguished the *taxon (behavioral orientation) system* for route navigation (a *taxis* is an organism's response to a stimulus by movement in a particular direction), and the *locale system* for map-based navigation and proposed that the locale system resides in the hippocampus. We have already qualified the latter assertion, showing how the hippocampus may function as *part of* a cognitive map. Here, we want to relate taxis to the notion of an affordance. Just as a rat may have basic taxes for approaching food or avoiding a bright light, say, so does it have a wider repertoire of affordances for possible actions associated with the immediate sensing of its environment. Such affordances include "go straight ahead" for visual sighting of a corridor, "hide" for a dark hole, "eat" for food as sensed generically, "drink", and the various turns afforded by, for example, the sight of the end of the corridor. Because the rat's behavior depends more on smell than on vision, we should add "olfactory affordances," but relevant data are sparse. Both normal and hippocampal-lesioned rats can learn to solve a simple T-maze in the absence of any consistent environmental cues other than the T-shape of the maze. If anything, the lesioned animals learn this problem faster than normals. After criterion was reached, probe trials with an eight-arm radial maze were interspersed with the usual T-trials. Animals from both groups consistently chose the side to which they were trained on the T-maze. However, many did not choose the 90° arm but preferred either the 45° or 135° arm, suggesting that the rats had solved the T-maze by learning to rotate within an egocentric orientation system at the choice point through *approximately* 90°. This leads to the hypothesis of an *orientation vector* being stored in the animal's brain but does not tell us where or how the orientation vector is stored. One possible model would employ coarse coding in a linear array of cells, coded for turns from −180° to +180°. From the behavior, one might expect that only the cells close to the preferred *behavioral* direction are excited and that learning "marches" this peak from the old to the new preferred direction. However, it requires a simpler learning scheme to "unlearn"−90°, say, by reducing the peak there, while at the same time "building" a new peak at the new direction of +90°. If the old peak has "mass" $p(t)$ and the new peak has "mass" $q(t)$, then as $p(t)$ declines toward 0 while $q(t)$ increases steadily from 0, the center of mass $\frac{(-90)p(t)+90q(t)}{p(t)+q(t)}$ will progress from −90 to +90, fitting the behavioral data.

The determination of movement direction is easily modeled by "rattification" of the Arbib and House (1987) model of frog detour behavior. There, prey were represented by excitation coarsely coded across a population, while barriers were encoded by inhibition whose extent closely matched the retinotopic extent of each barrier. The sum of excitation was passed through a winner-take-all circuit to yield the choice of movement direction. As a result, the direction of the gap closest to the prey, rather than the direction of the prey itself, was often chosen for the frog's initial movement. The same model serves for behavioral orientation once we replace the direction of the prey (frog) by the direction of the orientation vector (rat), while the barriers correspond to the absence of affordances for movement.

Hippocampal-Parietal Interactions in Navigation

McNaughton *et al.* (1989) found cells in rat posterior parietal cortex with location specificity that were dependent on visual input for their activation; 40% of the cells had responses discriminating whether the animal was turning left, turning right, or moving forward (we call these MLC cells). Some cells required a conjunction of movement and location (e.g., one parietal cell fired more for a right turn at the western arm of a cross-maze than for a right turn at the eastern arm), and these firings were far greater than for all left turns. Another parietal cell fired for left turns at the center of the maze but not for left turns at the ends of the arms or for any right turns. Turn-direction information was varied, with a given cell responding to a particular subset of vestibular input, neck and trunk proprioception, visual field motion, and (possibly) efference copy from motor commands.

McNaughton and Nadel (1990) offered a model of rat navigation with four components (Fig. 17a): B is a spatio-sensory input; A, in hippocampus, provides a place representation; L, posited to be parietal, outputs a movement representation; and AL provides a place/movement representation by means of the parietal MLC cells. In the model, A both transforms visual input from B into place cell activity and responds to input from AL by transforming the neural code of (prior place, movement) into that for the place where the rat will be after the movement. But this model becomes untenable, as MLC cells are *not* place/movement cells in the sense of

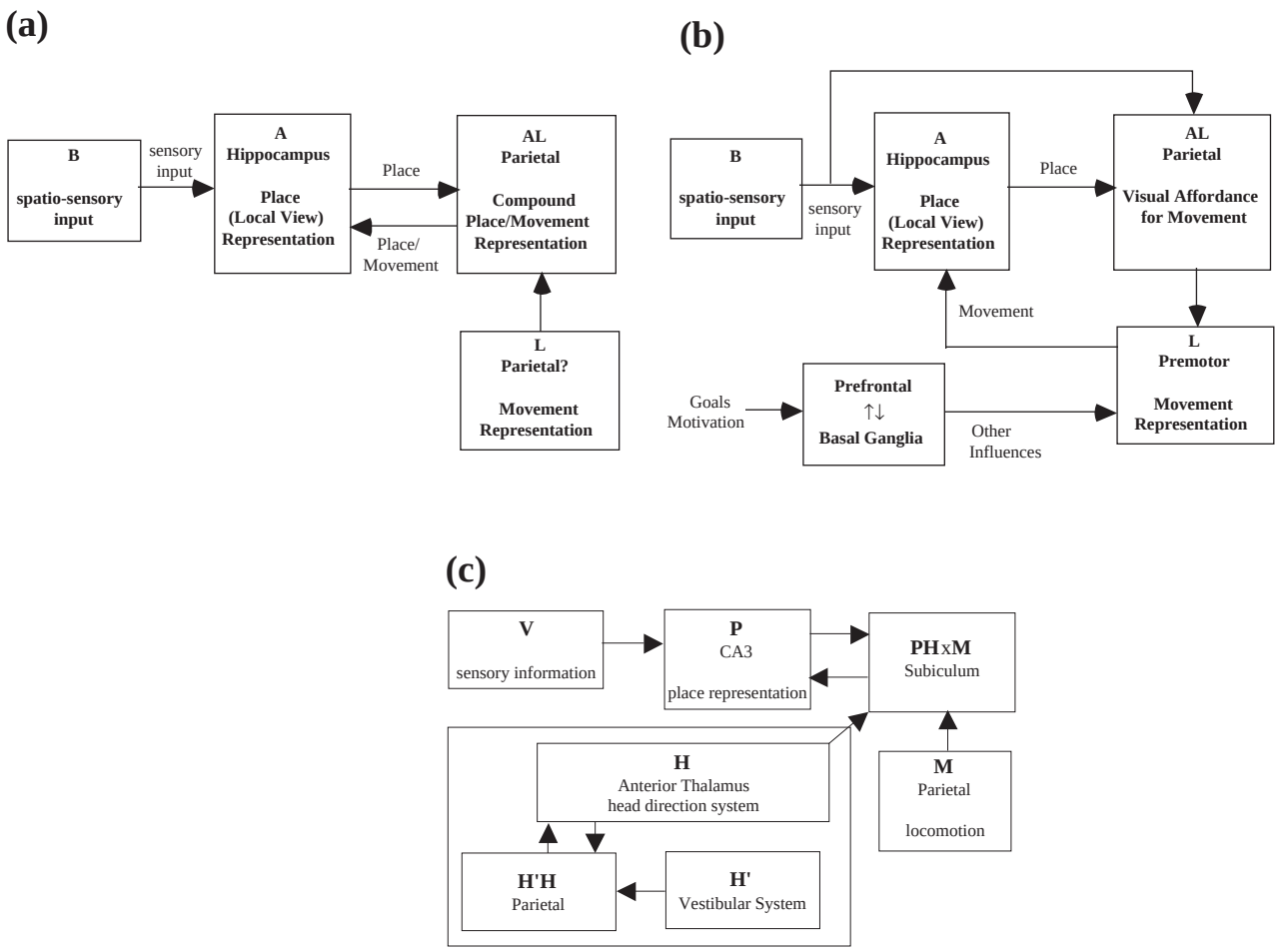

Figure 17 **(a)** A systems view of the role of hippocampus in spatially guided navigation (adapted from McNaughton and Nadel, 1990). **(b)** A recasting of the systems view of (a) which makes explicit that parietal cortex provides" "affordances" rather than explicit place information (ArbibÉá *et al*., 1997). **(c)** The McNaughton *et al*. 1996) systems-level view of the role of the hippocampus in navigation, redrawn from the perspective of (a).

"place" in "place cells." Examples of such a cell's "place/movement field" are "left turn at end of arm" or "move ahead along arm."

To proceed, we pursue analogies with monkey parietal cortex. We first *hypothesize* (for future experimental testing) that the parietal cortex of the rat also contains *affordance cells* for locomotion and navigation, akin to those documented in the monkey for reaching and grasping. Fig. 17b thus has the cells in AL (parietal cortex) code for affordances and includes a direct link from B to AL that is absent in Fig. 17a. Because "grip affordance cells" in AIP project to "grip premotor cells" in premotor region F5, we postulate analogously (Fig. 17b) that L is premotor and driven by AL. Once again, the current place is encoded in A, but we now posit that movement information from L enables A to compute the correct transformation from current place to next place. In either model, then, the loop via AL can, in absence of sensory input, update the place representation in A, with the cycle continuing until errors in this *expectation* accumulate excessively.

Fig. 17b also adds links from brain areas involved in goals and motivation – the navigation of a hungry rat is different than that of a sated rat. In analogy to the monkey, it posits (without further analysis) that interactions between prefrontal cortex and basal ganglia *choose* the rat's next movement on the basis of its current position relative to its goal. We shall say more of this when we discuss the World Graph model.

We now return to the MLC cells. Some fire prior to the rat's execution of a turn and correspond to the affordance cells of Fig. 17b, but others do not fire until the turn commences. These, then, are not signaling affordances, and we now describe a supplementary circuit (Paul Rothemund, USC term paper, Spring 1996) that includes our model of these cells. To ground this circuit, we turn to reports from the *monkey* literature of neurons that detect optic flow and have traces similar to those for MLC cells whose responses start at the initiation of a turn. These include MST neurons selective for expansion, contraction, and rotation (Graziao *et al*., 1994). Sakata *et al*. (1994) identified rotation-sensitive

(RS) neurons of the posterior parietal association cortex which, unlike MST neurons which seem specific for rotation in a fronto-parallel plane, were mostly sensitive to rotation in depth.

A neuron responding to a focus of expansion could seem to code for straight ahead, and a neuron encoding translational flow or rotation in depth could code for a turn. Some of the MLC cells which fire at a turn require head orientation in addition to visual input. We suggest that "parietal left turn" neurons combine input from an "MST left turn neuron" with vestibular input, efference copy, or somatosensory input. Such a "parietal left turn" neuron can thus function in the dark but does not code place as well as movement. A neuron that does code for a "place-specific left turn" might be constructed from a "parietal left turn" neuron and hippocampal input. We postulate that, though based on monkey data, this circuitry will (with different anatomical loci) be instantiated in rat brain, as well.

McNaughton *et al.* (1996) have proposed a new systems-level model that incorporates head direction information in the implementation of an angular path-integrator module. Note that head direction here is *not* absolute but is established with respect to sensory (e.g., visual) cues. It can be maintained moderately well if the animal moves in the dark but will be changed if the sensory cues are rearranged. Fig. 17c presents this model redrawn to emphasize its similarity with Fig. 17a. Box PHxM, previously PxM and assumed to be parietal, is now assumed to be implemented by the subiculum, based on the report by Sharp & and Green (1993) that some cells in the subiculum and dorsal presubiculum have broad, but significant, directional tuning in situations where directionality is absent from hippocampal cells.

McNaughton *et al.* (1996) view head direction as a point on a circle centered on the rat and assign each head-direction cell a location on this circle. This head-direction ring (H) has local Gaussian excitatory connections from a cell to its neighbors. Another layer of neurons (H′H) receives information about the current location from H and information about rotational motion from the vestibular system and other sources of such information (H′). These cells encode the interaction between current location and the sign of rotation and feed this information to cells on the appropriate side of the current focus of activity in the direction circle. Cells with these response properties have been observed in the rat posterior cortex (Chen *et al.*, 1994a,b). The posterior cortex is now assumed to implement the H′H system – which is almost identical to the dynamic remapping module postulated for LIP in the Dominey-Arbib model described before.

Taxon-Affordances (TAM) and World Graph (WG) Models

To move beyond these rather abstract diagrams, we developed two models of the rat navigational system (e.g., see Guazzelli *et al.*, 1998). The first, our TAM model of the rat's Taxon-Affordances system, explains data on the behavior of fornix-lesioned animals. The second, our World Graph (WG) model, explains data on the behavior of control rats and is also used for the study of cognitive maps. Together, these models shed light on the interactions between the taxon and locale systems and allow us to explain motivated spatial behavior. In order to describe both models, however, we first consider the notion of motivation and its implementation as a motivational schema with a dual role: setting current goals and providing.

So far, most models of spatial learning and navigation do not incorporate the role of motivation into their computation. By contrast, the WG theory (Arbib and Lieblich, 1977; Lieblich and Arbib, 1982) posits a set $d_1, d_2, \ldots, d_k$ of discrete drives to control the animal's behavior. At time t, each drive d_i in $(d_1, \ldots, d_k)$ has a value $d_i(t)$. The idea is that an appetitive drive spontaneously increases with time towards d_{max}, while aversive drives are reduced towards 0, both according to a factor *ad* intrinsic to the animal. An additional increase occurs if an incentive $I(d,x,t)$ is present, such as the aroma of food in the case of hunger. Drive reduction $a(d,x,t)$ takes place in the presence of some substrate – ingestion of water reduces the thirst drive. If the animal is at the place it recognizes as being node x at time t, and the value of drive d at that time is $d(t)$, then the value of d for the animal at time $t+1$ will be

$$d(t+1) = d(t) + a_d \mid d_{max} - d(t) \mid - a(d,x,t) \mid d(t) \mid + I(d,x,t) \mid d_{max} - d(t) \mid$$

which is the drive dynamics incorporated into the motivational schema.

Moreover, our motivational schema is not only involved in setting current goals for navigation; it is also involved in providing reinforcement for learning. Midbrain dopamine systems are crucially involved in motivational processes underlying the learning and execution of goal-directed behavior. Schultz *et al.* (1995) found that dopamine neurons in monkeys are uniformly activated by unpredicted appetitive stimuli such as food and liquid rewards and conditioned reward-predicting stimuli; they hypothesized that dopamine neurons may mediate the role of unexpected rewards to bring about learning. In our work, reward information is used to learn *expectations* of future reinforcements. Furthermore, the motivational schema implements the idea that the amount of reward is dependent on the current motivational state of the animal. If the rat is extremely hungry, the presence of food might be very rewarding, but, if not, it will be less and less rewarding. In this way, the influence of a reward $r(t)$ in TAM and the WG model will depend on the value of the animal's current dominant drive $d(t)$ (the maximum drive amongst all drives at a particular time t), its corres-

ponding maximum value, and the actual drive reduction, according to:

$$r(t) = \frac{d(t)}{d_{max}} a(d, x, t)$$

In this way, reward will bring about learning in the TAM and the WG models depending on the animal's current motivational state. On the other hand, if the rat reaches the end of a corridor and does not find food, the drive-reduction factor $a(d,x,t)$ is set equal to -0.1 times the normal value $a^*(d,x)$ it would have if food were present, and the motivational schema uses the above formula to generate a negative value of $r(t)$, a frustration factor, that will cause unlearning in TAM and in the WG model.

We have already outlined the basic ideas of the Taxon-Affordances model, based on the Arbib and House (1987) model of frog detour behavior. The full TAM model employs a reinforcement learning system, which tries to influence the behavior of the rat to maximize the sum of the reinforcement that will be received over time. However, rather than detailing the learning rule here, we turn to the World Graph model, which is rooted in the original model of Arbib and Lieblich (1977). In order to describe the WG model, we first describe the kinds of inputs presented to it, how these are processed, and how these inputs are finally incorporated into the model dynamics.

The WG model receives three kinds of inputs. These are given by three different systems: the place layer, the motivational schema, and the action selection schema. The WG model is composed of three distinct layers. The first layer contains coarse coded representations of the current sensory stimuli. This layer comprises four different perceptual schemas which are responsible for coding head direction, walls, and landmarks (bearings and distances), respectively. Perceptual schemas incorporate "what" and "where" information, the kind of information assumed to be extracted by the parietal and inferotemporal cortices (Kolb *et al.*, 1994; Mishkin *et al.*, 1983) to represent the perception of environmental landmarks and maze walls. In this model, perceptual schemas, like affordances, employ coarse coding in a linear one-dimensional array of cells to represent pertinent sensory input.

In the WG model, two distinct perceptual schemas are responsible for presenting landmark information to the network: one to code landmark bearing and the other to code landmark distance. However, because the experiments here are landmark free, the importance of landmarks for navigation and their further WG modeling will be described in another paper. Moreover, walls are also responsible for the formation of the rat's local view. O'Keefe and Burgess (1996) show place cells responsive to the walls of a box environment that modify their place fields in relation to different configurations of the environment. Muller and Kubie (1987) observed that, in some cases, place cells had a crescent-shaped field and were assumed to be related to the arena wall. In the WG model, if the wall is close to the rat (less than a body length in the current implementation), it will be represented in the "wall perceptual schema."

Cells that show a unimodal tuning to head direction independent of location and relative to a "compass direction" have been reported in several areas of the rat brain, including the post-subiculum (Taube *et al.*, 1990a,b) and the posterior parietal cortex, PPC (Chen *et al.*, 1994a,b). Head direction cells provide the animal with an internal representation of the direction of its motion. This information, like the other perceptual inputs in the WG model, will be coarse coded as a bump of activity over a linear array of cells, the head direction perceptual schema.

Each perceptual schema projects in turn to its respective feature detector layer. Each of these layers is organized in a two-dimensional matrix. Each node in the perceptual schema connects to all nodes in its corresponding feature detector layer (i.e., the two are fully connected). The feature detector units then interact through a local competition mechanism to contrast-enhance the incoming activity pattern; that is, a neuron in a feature detector layer produces a non-zero output (G_j) if and only if it is the most active neuron within a neighborhood. The adjustments to the connection weights between any pair of perceptual schema-feature detector layers are done using a normalized Hebbian learning algorithm. This ensures that the same set of feature detectors is activated by increasing the connection strength from active units (V_i) in the perceptual schema to active feature detectors, thereby increasing their response level the next time. This rule is captured in the following connection strength update equation:

$$\Delta_{w_{ij}} = \alpha V_i G_j w_{ij}$$

where Δw_{ij} is the change to the connection strength w_{ij} and α is the learning rate parameter.

Placed atop the feature detector layers is the Place Layer. This layer will keep track of the feature detector winners and will activate a different place/node if the set of winners that becomes active in the feature detector layers does not activate any previously activated node in the place layer. (The matching of winners is based on a pre-determined threshold.) In the WG theory, there is a node for each distinct place/situation the animal experiences. This is implemented in the WG model by a functional layer, called the World Graph layer, placed above the Place Layer. In this way, for each "new" set of feature detector winners, a "new" node is activated in the place layer and, consequently, a node x is created in the world graph layer of the WG model.

In the WG theory, there is an edge from node x to node x' in the graph for each distinct and direct path the animal has traversed between a place it recognizes as x

and a place it recognizes as x'. This is implemented in the WG model as a link between two nodes of the World Graph layer. Suppose, for example, a node x is currently active at time t. By deciding to move north, the animal activates a "different" set of feature detectors and so a distinct node x' in the world graph at time $t+1$, and a link will be created from node x to node x'. Appended to each link/edge will be sensorimotor features associated with the corresponding movement/path. In the current model, these features consist of a motor efference copy (e.g., movement towards north) supplied to the world graph via a feedback connection from the action selection schema.

Edge information allows the animal to perform goal-oriented behaviors. The WG model learns expectations of future reward by the use of temporal differences learning in an actor-critic architecture (Barto *et al.*, 1983; Sutton, 1988). Expectations of future reinforcement are associated with pairs of nodes/edges, not with state/actions as is the case in TAM. For this reason, when a particular node of the world graph is active and, for example, the simulated animal is hungry, all it needs to do is select the edge containing the biggest hunger-reduction expectation and follow its direction toward the node it points to. In the WG model, each drive will have an associated drive-reduction expectation value. Thus, if the rat is thirsty, it will not base next node selection on hunger-reduction expectations, but on thirst-reduction expectations.

The integrated model, TAM-WG, joins together TAM and the WG model. The result is depicted in Fig. 18. In TAM-WG, the decision to turn to a certain angle (the orientation vector) is given by a winner-take-all process performed over the integration of fields produced by the available affordances (AF), drive-relevant stimuli (ST), rewardness expectation (RE), map information from the world graph (MI), and a curiosity level (CL) – to be described below. MI, as well as RE, contains an associated noise factor – *noise_mi*. If a node x is active in the world graph, there will be expectations associated with each edge coming from node x. Because associated with each edge is the direction it points to, a peak of activity with the magnitude of the expectation associated with that node/edge pair will be coarse coded over a linear array of neurons in the location respective to the edge's direction. In TAM-WG, then, the total input I_{in} to the action selection schema becomes:

$$I_{in}(i,t) = AF(i,t) + ST(i,t) + (RE(i,t) + noise\_re) + (MI(i,t) + noise\_mi) + CL(i,t)$$

Eventually, the selected motor outputs will enable the system to reach the goal object. When a selected action is executed, it will produce consequences in the animal's internal state and in the way it perceives the world (*cf.* the action-perception cycle; Arbib, 1972). The internal state will alter the drive levels, which will in turn influence the selection of the next node in the world graph, and so on.

A crucial aspect of the WG theory and the TAM-WG model is that an animal may go to places that are not yet represented in its world graph. To see how this occurs, we must clarify what is meant by a node x' immediately adjacent to a node x. Certainly, if there is an edge from x to x' in the world graph, then x' is immediately adjacent to x. However, the WG theory also considers as adjacent to x those world situations x' not yet represented in the graph, but that can be reached by taking some path from x. In the WG model, these situations will have a value attached to them, which can be seen as a "curiosity level" attached to the unknown. The curiosity level is based on the value of the animal's biggest drive at a particular given time.

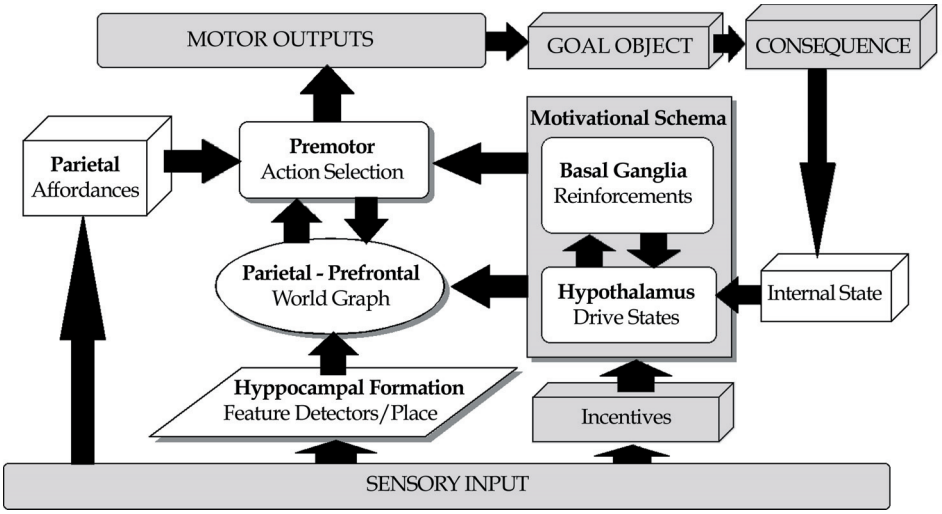

Figure 18 Integrated TAM-WG model of rat navigation.

2.1.6 Discussion

Chapter 2.2 presents the NSL Neural Simulation Language which (whether in earlier or current versions) has been the vehicle for much of the modeling at the level of systems neuroscience discussed in this chapter. It should be noted that the NSL of Chapter 2.2 is NSLJ, an implementation of NSL 3.0 in Java which extends the object-oriented approach implemented in C++ for NSL 2.1. Because the development of the models reported in this chapter was contemporaneous with the development of NSLJ, the current implementations of these models reflect this heterogeneity – they are implemented in NSL2.1 or NSLJ, C++ or Java. However, all are being re-implemented into NSLJ or, at least, into a form that will allow the modular description and links to data that test and support the model which will be offered by the Brain Models on the Web (BMW) model repository (Chapter 6.2). BMW provides documentation, links to empirical data, and downloadable code for almost all the models described in this chapter. Chapter 2.4 presents the Synthetic PET method, which provides the bridge from such neural-level modeling, grounded in the data of animal neurophysiology, to the data of human brain imaging.

Much attention has been paid by other groups to multi-compartment modeling (e.g., the GENESIS and NEURON neural simulation environments) using the Hodgkin-Huxley equation and detailed models of receptor kinetics and plasticity to model membrane properties in dendrite, soma, and axon to help us understand small neural circuits. One of the goals for future work by the USC Brain Project is to develop a set of BMW Standards so that many different neural simulation environments (NSL, GENESIS, NEURON, etc.) can have their models structured for inclusion in BMW.

Another effort of the USC Brain Project has focused on modeling at an even finer level than that provided by either GENESIS and NEURON. Chapter 2.3 will present the work on EONS (Elementary Objects of the Nervous System), with particular attention to EONS models of synapses and the fine structures which constitute them. Not only can EONS simulations take into account the position of transmitter release and the position of receptor macromolecules, but they can also accommodate the irregular geometry of the pre- and postsynaptic membranes based on electron micrograph data.

Acknowledgments

This work was supported in part by a Program Project (P20) grant from the Human Brain Project (P01MH52194) and in part by the National Science Foundation (IRI-9221582). My thanks to Peter Dominey, Michael Crowley, and Amanda Bischoff-Grethe for their work on modeling the basal ganglia and to Tom McNeill (a founding faculty member of USCBP) for his unfailing counsel during the development of these models; to Nicolas Schweighofer and Jacob Spoelstra for their work on modeling the cerebellum and to Tom Thach for discussion of relevant empirical data; to Andrew Fagg for his work on the FARS model and to Giacomo Rizzolatti and Hideo Sakata for their discussion of relevant data; to Paul Rothemund for suggesting the role in navigation of parietal systems for detection of visual motion; and to Alex Guazzelli, Mihail Bota, and Fernando Corbacho for valuable discussion on the linkage of hippocampus to other systems in the control of navigation.

References

Agostino, A., Berardelli, A., Formica, A., Accornero, N., and Manfredi, M. (1992). Sequential arm movements in patients with Parkinson's disease, Huntington's disease and dystonia. *Brain* **115,** 1481–1495.

Aitkin, L. M., and Boyd, J. (1978). Acoustic input to the lateral pontine nuclei. *Hearing Res.* **1**, 67–77.

Albus, J. (1971). A theory of cerebellar function. *Mathematical Biosci.* **10**, 25–61.

Arbib, M. A. (1997). From visual affordances in monkey parietal cortex to hippocampo-parietal interactions underlying rat navigation. *Phil. Trans. R. Soc. London B*. **352**, 1429–1436.

Arbib, M. A., Ed. (1995). *The Handbook of Brain Theory and Neural Networks*. Bradford Books/The MIT Press, Cambridge, MA.

Arbib, M. A. (1981). Perceptual structures and distributed motor control. In *Handbook of Physiology, Section 2*. The Nervous System. Vol. II. *Motor Control, Part 1* (V. B. Brooks, Ed.). American Physiological Society, pp. 1449–1480.

Arbib, M. A. (1972). *The Metaphorical Brain*. Cybernetics as Artificial Intelligence and Brain Theory. Wiley-Interscience, New York.

Arbib, M. A., and House, D. H. (1987). Depth and detours, an essay on visually-guided behavior. In *Vision, Brain, and Cooperative Computation* (Arbib, M. A., and Hanson, A. R. Eds.). A Bradford Book/The MIT Press, Cambridge, MA, pp. 129–163.

Arbib, M. A., and Lieblich, I. (1977). Motivational learning of spatial behavior. In *Systems Neuroscience*. (Metzler, J. Ed.). Academic Press, New York, pp. 221–239.

Arbib, M. A., Érdi, P., and Szentágothai, J. (1998). *Neural Organization*: Structure, Function and Dynamics. A Bradford Book/The MIT Press, Cambridge, MA.

Arbib, M. A., Schweighofer, N., and Thach, W. T. (1995). Modeling the Cerebellum: From Adaptation to Coordination, in *Motor Control and Sensory-Motor Integration*: Issues and Directions (Glencross, D. J., and Piek, J. P., Eds.). North-Holland Elsevier Science, Amsterdam, pp. 11–36.

Arbib, M. A., Schweighofer, N., and Thach, W. (1994). Modeling the role of cerebellum in prism adaptation. In *From Animals to Animats 3* (Cliff, D., Husbands, P., Meyers, J., and Wilson, S., Eds.). The MIT Press, Cambridge, MA, pp. 36–44.

Arbib, M. A., Boylls, C. C., and Dev, P. (1974). Neural models of spatial perception and the control of movement. In *Kybernetik und Bionik/Cybernetics* (Oldenbourg, R., Ed.). pp. 216–231.

Bal, T., and McCormick, D. A. (1996). What stops synchronized thalamocortical oscillations? *Neuron.* **17**, 297–308.

Barone, P., and Joseph, J.-P. (1989). Prefrontal cortex and spatial sequencing in macaque monkey. *Exp. Brain Res.* **78**, 447–464.

Bartha, G., and Thompson, R. (1995). Cerebellum and conditioning. In *The Handbook of Brain Theory and Neural Networks* (Arbib, M. A., Ed.). The MIT Press, Cambridge, MA, pp. 169–172.

Barto, A. G., Richard, S., and Anderson, C. W. (1983). Neuronlike adaptive elements that can solve difficult learning control problems. *IEEE Trans. Systems, Man, Cybernetics*, SMC-**13**, 834–846.

Berthier, N. W., and Moore, J. W. (1986). Cerebellar Purkinje cell activity related to the classically conditioned nictitating membrane response. *Exp. Brain Res.* **63**, 341–350.

Bischoff, A. (1998). Modeling the Basal Ganglia in the Control of Arm Movements, Ph. D. thesis, Department of Computer Science, University of Southern California, Los Angeles.

Bischoff-Grethe, A., and Arbib, M. A. (2000). Sequential movements: a computational model of the roles of the basal ganglia and the supplementary motor area.

Borges, J. L. (1975). Of exactitude in science. In *A Universal History of Infamy* Penguin Books, New York, p. 131,.

Bronstein A,M., and Kennard, C. (1985). Predictive ocular motor control in Parkinson's disease. *Brain* **108**, 925–940.

Buford, J. A., Inase, M., and Anderson, M. E. (1996). Contrasting locations of pallidal-receiving neurons and microexcitable zones in primate thalamus. *J. Neurophysiol.* **75**, 1105–1116.

Chen, L. L., Lin, L. H., Green, E. J., Barnes, C. A., and McNaughton, B. L. (1994a). Head-direction cells in the rat posterior cortex. 1. Anatomical distribution and behavioral modulation. *Exp. Brain Res.* **101(1)**, 8–23.

Chen, L. L., Lin, L. H., Barnes, C. A., and McNaughton, B. L. (1994b). Head-direction cells in the rat posterior cortex. 2. Contributions of visual and ideothetic information to the directional firing. *Exp. Brain Res.* **101(1)**, 24–34.

Crowley, M. (1997). Modeling Saccadic Motor Control: Normal Function, Sensory Remapping and Basal Ganglia Dysfunction, Ph. D. thesis, Department of Computer Science, University of Southern California, Los Angeles.

Curra, A., A. Berardelli, R. Agostino, N. Modugno, C. C. Puorger, N. Accornero, and M. Manfredi (1997). Performance of sequential arm movements with and without advance knowledge of motor pathways in Parkinson's disease. *Movement Disord.* **12**, 646–654.

Dominey, P. F., and Arbib, M. A. (1992). A cortico-subcortical model for generation of spatially accurate sequential saccades. *Cerebral Cortex.* **2**, 135–175.

Eccles, J. C., Faber, D. S., Murphy, J. T., Sabah, N. H., and Táboríková, H. (1971). Afferent volleys in limb nerves influencing impulse discharge in cerebellar cortex. I. In mossy fibers and granule cells. *Exp. Brain Res.* **1**, 1–16.

Eccles, J. C., Ito, M., and Szentágothai, J. (1967). *The Cerebellum as a Neuronal Machine*. Springer-Verlag, Berlin.

Eichenbaum, H., Kuperstein, M., Fagan, A., and Nagode, J. (1987). Cue-sampling and goal-approach correlates of hippocampal unit activity in rats performing an odor-discrimination task. *J. Neurosci.* **7**, 716–732.

Fagg, A. H., and Arbib, M. A. (1998). Modeling parietal-premotor interactions in primate control of grasping. *Neural Networks* **11**, 1277–1303.

Georgopoulos, A., Kettner, R., and Schwartz, A. (1988). Primate motor cortex and free arm movements to visual targets in three-dimensional space. II. Coding of the direction of movement by a neuronal populaion. *J. Neurosci.* **8**, 2928–2937.

Gibson, J. J. (1979). *The Ecological Approach to Visual Perception.* Houghton Mifflin, Boston, MA.

Graziao, M. S. A., Andersen, R. A., and Snowden, R. J. (1994). Selectivity of area MST neurons for expansion, contraction, and rotation motions. *Invest. Ophthalmol. Visual Sci.* **32**, 823–882.

Grethe, J. S. (1999). Neuroinformatics and the Cerebellum: Towards an Understanding of the Cerebellar Microzone and Its Contribution to the Well-Timed Classically Conditioned Eyeblink Response, Doctoral dissertation, University of Southern California, Los Angeles.

Guazzelli, A., Corbacho, F. J., Bota, M., and Arbib, M. A. (1998). Affordances, motivation, and the World Graph theory. *Adaptive Behav.* **6**, 435–471.

Hoff, B., and Arbib, M. A. (1992). A model of the effects of speed, accuracy, and perturbation on visually guided reaching. In *Control of Arm Movement in Space, Neurophysiological and Computational Approaches*. (Caminiti, R., Johnson, P. B., and Burnod, Y., Eds.), Springer-Verlag, Berlin.

Humphrey, D. (1979). The cortical control of reaching. In *Posture and Movement*. (Humphrey, D. R. and Talbot, D., Eds.). Raven Press, New York, pp. 51–112.

Ito, M. (1984). *The Cerebellum and Neural Control*. Raven Press, New York.

Jeannerod, M., Arbib, M. A., Rizzolatti, G., and Sakata, H. (1995). Grasping objects: the cortical mechanisms of visuomotor transformation. *Trends Neurosci.* **18**, 314–320.

Jenkins, I. H., Brooks, D. J., Nixon, P. D., Frackowiak, R. S. J., and Passingham, R. E. (1994). Motor sequence learning: a study with positron emission tomography. *J. Neurosci.* **14**, 3775–3790.

Kaplan, S., Sonntag, M., and Chown, E. (1991). Tracing recurrent activity in cognitive elements (TRACE): a model of temporal dynamics in a cell assembly. *Connection Sci.* **3(2)**, 179–206.

Kolb, B., Buhrmann, K., McDonald, R. and Sutherland, R. J. (1994). Dissociation of the medial prefrontal, posterior parietal, and posterior temporal cortex for spatial navigation and recognition memory in the rat. *Cerebral Cortex*. **4(6)**, 664–680.

Lashley K. S. (1951). The problem of serial order in behavior. In *Cerebral Mechanisms in Behavior*. (Jeffress, L. A., Ed.). John Wiley & Sons, New York, pp. 112–146.

Lieblich, I., and Arbib, M. A. (1982). Multiple representations of space underlying behavior. *Behavioral Brain Sci.* **5**, 627–659.

Llinás, R. R., and Mühlethaler, M. (1988). Electrophysiology of guinea-pig cerebellar nuclear cells in the *in vitro* brainstem cerebellar preparation. *J. Physiol.* **404**, 241–258.

Luppino, G., Matelli, M., Camarda, R., and Rizzolatti, G. (1993). Corticocortical connections of area F3 (SMA-proper). and area F6 (pre-SMA). in the macaque monkey. *J. Comp. Neurol.* **338**, 114–140.

Marr, D. (1969). A theory of cerebellar cortex. *J. Physiol.* **202**, 437–470.

Martin, T., Keating, J., Goodkin, H., Bastian, A., and Thach, W. (1996). Throwing while looking through prisms. 1. Focal olivocerebellar lesions impair adaptation. *Brain* **119(suppl. 4)**, 1183–1198.

Martin, T., Keating, J., Goodkin, H., Bastian, A., and Thach, W. (1995). Throwing while looking through prisms. 1. Focal olivocerebellar lesions impair adaptation. *Brain* **119(suppl. 4)**, *1183–1198.*

McNaughton, B. L., and Nadel, L. (1990). Hebb-Marr networks and the neurobiological representation of action in space. In *Neuroscience and Connectionist Theory*. (Gluck, M. A., and Rumelhart, D. E., Eds.). Lawrence Erlbaum Assoc., Norwood, NJ, chap. 1, pp. 1–63.

McNaughton, B. L., Barnes, C. A., Gerrard, J. L., Gothard, K., Jung, M. W., Knierim, J. J., Kudrimoti, H., Qin, Y., Skaggs, W. E., Suster, M., and Weaver, K. L. (1996). Deciphering the hippocampal polyglot: the hippocampus as a path integration system. *J. Exp. Biol.* **199(pt. 1)**, 173–185.

McNaughton, B. L., Leonard, B., and Chen, L. (1989). Cortico-hippocampal interactions and cognitive mapping: a hypothesis based on reintegration of the parietal and inferotemporal pathways for visual processing. *Psychobiology* **17**, 230–235.

Mishkin, M., Ungerleider, L. G., and Mack, K. A. (1983). Object vision and spatial vision: two cortical pathways. *Trends Neurosci.* **6**, 414–417.

Muller, R. U., and Kubie, J. L. (1987). The effects of changes in the environment on the spatial firing of hippocampal complex-spike cells. *J. Neurosci.* **7(7)**, 1951–1968.

O'Keefe, J., and Burgess, N. (1996). Geometric determinants of the place fields of hippocampal neurons. *Nature* **381(6581)**, 425–8.

O'Keefe, J., and Conway, D. H. (1978). Hippocampal place units in the freely moving rat: why they fire when they fire. *Exp. Brain Res.* **31**, 573–590.

O'Keefe, J., and Dostrovsky, J. (1971). The hippocampus as a spatial map: preliminary evidence from unit activity in the freely moving rat. *Exp. Brain Res.* **34**, 171–175.

O'Keefe, J., and Nadel, L. (1978). *The Hippocampus as a Cognitive Map*. Clarendon Press, Oxford.

Ranck, J. B. (1973). Studies on single neurons in dorsal hippocampal formation and septum in unrestrained rats. I. Behavioral correlates and firing repertoires. *Exp. Neurol.* **41**, 461–535.

Rizzolatti, G., Camarda, R., Fogassi, L., Gentilucci, M., Luppino, G., and Matelli, M. (1988). Functional organization of inferior area 6 in the Macaque monkey. II. Area F5 and the control of distal movements. *Exp. Brain Res.* **71**, 491–507.

Robinson, D. A. (1981). The use of control systems analysis in the neurophysiology of eye movements. *Ann. Rev. Neurosci.* **4**, 463–503.

Sakata, H., Shibutani, H., Ito, Y., Tsurugai, K., Mine, S., and Kusunoki, M. (1994). Functional properties of rotation-sensitive neurons in the posterior parietal association cortex of the monkey. *Exp. Brain Res.* **101(2)**, 183–202.

Schultz, W., Romo, R., Ljungberg, T., Mirenowicz, J., Hollerman, J. R., and Dickinson, A. (1995). Reward-related signals carried by dopamine neurons. In *Models of Information Processing in the Basal Ganglia*. (Houk, J. R., *et al.*, (Eds.). The MIT Press, Cambridge, MA, pp. 233–248.

Schweighofer, N., Arbib, M. A., and Kawato, M. (1998a). Role of the cerebellum in reaching quickly and accurately. I. A functional anatomical model of dynamics control. *Eur. J. Neurosci.* **10**, 86–94.

Schweighofer, N., Spoelstra, J., Arbib, M. A., and Kawato, M. (1998b). Role of the cerebellum in reaching quickly and accurately. II. A detailed model of the intermediate cerebellum, *Eur. J. Neurosci.* **10**, 95–105.

Schweighofer, S., Arbib, M. A., and Dominey, P. F. (1996a). A Model of Adaptive Control of Saccades: I. The model and its biological substrate. *Biol. Cybernetics* **75**, 19–28.

Schweighofer, S., Arbib, M. A., and Dominey, P. F. (1996b). A model of adaptive control of saccades. II. Simulation results. *Biol. Cybernetics* **75**, 29–36.

Scudder, C. A. (1988). A new local feedback model of the saccadic burst generator. *J. Neurophysiol.* **59**, 1455–1475.

Sharp, P. E., and Green, C. (1994). Spatial correlates of firing patterns of single cells in the subiculum of the freely moving rat. *J. Neurosci.* **14**, 2339–2356.

Spoelstra, J., and Arbib, M. A. (1997). A computational model of the role of the cerebellum in adapting to throwing while wearing wedge prism glasses. In *Proceedings of the 4th Joint Symposium on Neural Computation*. Vol. 7. Los Angeles, CA, pp. 201–208.

Spoelstra, J., Arbib, M. A., and N. Schweighofer (2000). Cerebellar control of a simulated biomimetic manipulator for fast movements. *Biol. Cybernetics*, in press.

Steinmetz, J. E. (1990). Classical nictitating membrane conditioning in rabbits with varying interstimulus intervals and direct activation of cerebellar mossy fibers as the CS. *Behav. Brain Res.* **38**, 97–108.

Sutton, R. (1988). Learning to predict by the methods of temporal differences. *Machine Learning* **3**, 9–44.

Taira, M., S. Mine, Georgopoulos, A. P., Murata, A., and Sakata, H. (1990). Parietal cortex neurons of the monkey related to the visual guidance of hand movement. *Exp. Brain Res.* **83**, 29–36.

Tanji, J., and Shima, K. (1994). Role for supplementary motor area cells in planning several movements ahead. *Nature* **371**, 413–416.

Taube, J. S., Muller, R. U., and Ranck, J. B. Jr. (1990a). Head-direction cells recorded from the postsubiculum in freely moving rats. I. Description and quantitative analysis. *J. Neurosci.* **10**, 420–435.

Taube, J. S., Muller, R. U., and Ranck, J. B. Jr. (1990b). Head-direction cells recorded from the postsubiculum in freely moving rats. II. Effects of environmental manipulations. *J. Neurosci.* **10(2)**, 436–47.